ESCUELA POLITÉCNICA SUPERIOR DE MONDRAGON UNIBERTSITATEA
MONDRAGON UNIBERTSITATEKO GOI ESKOLA POLITEKNIKOA

Trabajo fin de máster presentado para la obtención del título de *Titulua eskuratzeko master bukaerako lana*

MÁSTER UNIVERSITARIO EN TECNOLOGÍAS BIOMÉDICAS
TEKNOLOGIA BIOMEDIKOEN UNIBERTSITATE MASTERRA

Título del Trabajo *Lanaren izenburua*

Development of a standardized and automated device for the quantification of neural cell response to impact

Autor *Egilea* ANDONI IZAGUIRRE ARRIETA

Curso *Ikasturtea* 2021/2022

Título del Trabajo *Lanaren izenburua*

Development of a standardized and automated device for the quantification of neural cell response to impact

Nombre y apellidos del autor
Egilearen izen-abizenak
ARRIETA IZAGUIRRE, ANDONI

Nombre y apellidos del/los director/es del trabajo
Zuzendariaren/zuzendarien izen-abizenak
TADRIST, LOÏC
ARRAZOLA, PEDRO JOSE

Lugar donde se realiza el trabajo
Lana egin deneko lekua
Aix Marseille Université

Curso académico
Ikasturtea
2021/2022

Abstract

In this master's final project, a standardized and automated device for the quantification of neural cell response to impact was developed. The impact device was designed to produce impacts in vertical orientation with on-demand maximal acceleration and contact time. Requirements were to create a robust device that supports repeated impacts. Firstly, analytical and computational analysis were performed to check the theoretical behaviour of the device. Hertz impact model equations were used to set primary functionality of the device as well as for dimensioning of the target elements (bumper). Computational analysis was performed via finite element modelling (FEM) with 3D Experience platform. The device was validated reproducing experimental test and matching theoretical results with experimental ones. A low-cost compact device was manufactured, being easy to manipulate and with high reproducibility capacity.

Resumen

En este proyecto final de máster, se ha desarrollado un dispositivo estandarizado y automatizado para la cuantificación de la respuesta de las células neurales ante impactos. El dispositivo de impacto se ha diseñado para producir impactos en orientación vertical en demanda de analizar las aceleraciones máximas y el tiempo de contacto. Los requisitos han sido crear un dispositivo robusto capaz de soportas repetidos test de impactos. En primer lugar, se han realizado análisis analíticos y computacionales para comprobar el comportamiento teórico del dispositivo. Se han utilizado las ecuaciones del modelo de impacto de Hertz para establecer la funcionalidad primaria del dispositivo, así como para el dimensionamiento de los elementos primordiales (parachoques). El análisis computacional se ha realizado mediante la modelización de elementos finitos (FEM) con la plataforma 3D Experience. El dispositivo se ha validado experimentalmente, haciendo coincidir los resultados teóricos con los test reales. Se ha conseguido fabricar un dispositivo compacto de bajo coste, fácil de manipular y con gran capacidad de reproducibilidad.

Laburpena

Master bukaerako proiektu hontan, impaktu mekaniko ezberdinen aurrean zelula neuronalek izan ditzaketen efektuak aztertzeko gailu estandarizatu eta automatizatu bat sortu da. Gailu hau, impaktuak orientazio bertikalean jasateko diseinatua izan da, azelerazio eta kontaktu denbora neurtzeko asmotan. Baldintza nagusi bat, impaktu errepikatuak jasateko prestatua egota izan da. Horretarako, analisi analitiko zein komputazionalak bideratu dira, gailu berriaren izaera teorikoa frogatzeko asmoz. Gauluaren funtzionamendu primarioa zein impaktuetan erabiliko diren "bumper" ezberdinen dimentsionamendurako Hertz impaktu modeloen ekuazioak erabili dira. Analisi konputazionalak element finituen modeloak (FEM) erabiliz aztertu dira. Hauek, 3D Experience plataforman oinarrituz sortu dira. Azkenik, gailua experimentalki balidatu da, aurretik jorratutako analisi analitiko zein konpitazionalekin konparatuz eta honen funtzionamendu erreala teoriarekin aztertuz. Horrela, gailu prezio baxuko gailu konpaktu bat sortzea lortu da, erabiltzeko errextasuna zein experimendu reprodukzio handia ahalbidetzen duena.

Glossary

E	Young's modulus of the material
R	Radius of curvature of the bumper
u_0	Impact velocity
δ_{max}	Penetration depth
$\ddot{\delta}$	Maximum acceleration
T_c	Contact time
m	Mass
g	Gravity
h	Height
T_c^A	Analytic contact time
T_c^S	Simulation contact time
$\ddot{\delta}_A$	Analytic maximum acceleration
$\ddot{\delta}_S$	Simulation maximum acceleration
α	Pre-factor for maximal acceleration model
β	Pre-factor for contact time model

Index

Table des matières

List of figures

List of tables

1. Introduction

Brain damages consecutives to head impacts cannot be diagnosed immediately. This results in an underestimation of trauma severity and renewed risk-taking before recovery. For now, there is no effective therapeutic treatment or solution for traumatic brain injury (TBI), being even more urgent to improve and develop new prevention devices as proposed ion this project.

1.1 State of the art

1.1.1 Why we study impacts on cells?

Traumatic brain injury (TBI) is one of the highest leading causes of death in the last decade[1] becoming even more significant issue in public health. Known as "an alteration in brain function, or other evidence of brain pathology, caused by an external force"[1] is still a complex and barely understood global disease.

Received impacts transfer mechanical energy to the brain which reduces its functionality, where depending on the magnitude of the external force, injury varies in different levels. TBI can be classified as mild, moderate and severe. This classification is based on clinical observations of an injured brain functionality. So far, criteria for biological quantification are determined by the Glasgow Coma Scale [2]. However, this injury indicators come with limitations not providing consistent evaluations for same patient. As well, it is difficult to verify the magnitude of the trauma in terms of energy transfer [3]. Therefore, it is essential to perform an injury classification by energy transfer mechanisms in terms of low, moderate or high energy transfer impacts. This kind of classification supposes and ease for attention in general trauma care and helps on-scene trauma triage.

New study performed by Lecky et al. tried to conduct a cohort study comparing TBI patients injured by low-energy transfer (LE cohort) to high-energy transfer (HE cohort). Derived by CENTER-TBI (Collaborative European NeuroTrauma Effectiveness Research in TBI) registry for patients between 2014 and 2018 were used. TBI indicators were obtained from computed tomography (CT) brain scan samples. Overall, the study recollects patient demographics, injury, care pathway, and other outcome data over

18 European countries (17 countries in Europe and Israel) as depicted in table 1 and table 2. 21681 TBI patients presenting injury mechanism were analyses. 40% (8622/21681) were injured by LE transfer compared to 60% (13059/21681) by HE transfers. Eventually, those injured by LE were older (median 74 years) and often female compared to HE (median 42 years). Study show that patients injured by LE less often presented moderate to severe impair conscious levels but had similar in-hospital mortality rate (LE 6,3% versus HE 7,0%). This comes from LE injured patients were 50 % less likely to receive critical care (LE 12% versus HE 24% or emergency interventions (LE 7,5% versus HE 13%).

Characteristics	**Overall**	**HE TBI**	**LE TBI**
n patients	21,681	13,059	8,622
Age	55 (32-75)	42 (25-60)	74 (56-84)
Place of injury			
Street/Highway	33.8	48.5	11.6
Home/Domestic	38.3	21.9	63.0
Sports	3.3	5.1	0.6
Public location	15.7	15.3	16.2
Work/School	3.4	4.5	1.8
Other	5.6	4.7	6.9
GCS			
Mild TBI (GSC 13-15)	81.6	78.6	86.2
Moderate TBI (GSC 9-12)	3.8	3.7	4.1
Severe TBI (GSC 3-8)	5.5	6.7	3.7

Data are in (%) unless indicated; GSC, Glasgow Coma Score

Table 1: LE and HE cohort study derived by TBI-CENTER. Observed data of patients is classified by different scenarios and GSC score. Depicted data is given in % over number of studied patients.

Characteristics	Overall	HE TBI	LE TBI
Care pathway			
Emergency dept.	9286 (42.8)	5511 (42.2)	3775 (43.8)
Hospitalized	38	33	45
ICU	19.2	24.4	11
CT characteristics			
Abnormal CT	6746 (31.1)	4226 (32.4)	2520 (29.2)
EDH	12.7	14.9	9
ASDH	44.8	42.4	48.8
Contusions	44.7	49.8	36.3
Subarachnoid haemorrhage	52	56.7	44.1
III Diffuse injury	22.8	1.4	0.4
IV Diffuse injury	1	0.8	1.1
Mortality and discharge			
Hospital mortality	1453 (6.7)	913 (7)	540 (6.3)
Discharged home	15324 (70.7)	9458 (72.2)	5866 (68)
Rehabilitation	1221 (5.6)	776 (5.9)	445 (5.2)

Data are in (%) unless indicated; ICU, intensive care unit; CT, computed tomography; EDH, extradural haematoma; ASDH, acute subdural haematoma

Table 2: LE and HE cohort study derived by TBI-CENTER. Observed data is classified by care pathway given to patients and injury characteristics they present. As well, mortality and discharged data is included. Depicted data is given in % over number of studied patients

Moreover, evidence showing relation between repeated mild traumatic brain injury within long-term neurodegenerative disorders, studies have found that the behaviour of TBI could be both an acute disorder and chronic disease [4], [5]. However, there is still a lack of understanding on how to analyse milder forms of injury, from moderate to severe TBI, such as concussions or those that can create intracranial injuries.

At this point, TBI has an important public health burden, where those injured by high-energy transfer such as road traffic collisions (RTC) or high-level falls are assumed to

create more severe injuries. These cases are prioritised by medical emergency attention; however, recent investigation suggest an important increase in people injured through low to moderate energy transfers (i.e., low level falls) which derived in severe health issues on patients. It is necessary to study which is the effect of different energy level transfer of TBI to recopilate new data of patients injured by TBI impacts.

For that, a primary classification has been made to characterize energy level transfers with different kind of possible scenarios (Table 3). Based on mean values for impact velocities that can affect in those scenarios [6], classification has been adapted in function of some estimated height values. In terms of energy, it is possible to identify and classify each scenario for different levels.

Energy transfer level	Scenario	Velocity (m/s)	Height (m)	Energy (J)
Low energy	Standing	0-1	Human Height	88
Moderate Energy	Low Level Fall	0-1	1-2	98.1
	Medium Level Fall	0-1	2-3	147.15
	Sports (hitting ball)	4-6	-	90
High Energy	Sports, collision	8-10	-	250
	RTC	>11	-	>562.5
	High Level Fall	0-1	>3	>147.15
	Blunt assault	>9	-	>250
	High risk sorts, Athleticism	>6	-	>90

Table 3: Primary classification of energy transfer level. Possible different scenarios have been determined. Characterization of energy level is given in function of estimated velocities, height, and energy quantity.

This classification could be useful to determine severity of injuries in advance. Furthermore, the criteria may help in future TBI studies to focus specific performances in terms of energy transfer level and develop new research path in this field.

1.1.2 Medical methods to analyse TBI

TBI occurs by an external mechanical stimulus resulting in both mechanical, i.e., deformation of the brain tissue after first injury, and biological, i.e., inflammatory response or cell death. This is observed analysing biological effects occurred within the central nervous system (CNS). Moreover, main effects have been studied controlling the behaviour of astrocytes. Located near to neurons and blood vessels in the brain, astrocytes are most abundant glial cells in CNS. They compound the blood-brain barrier, transporting essential molecules and nutrients to neurons (Figure 1) [7].

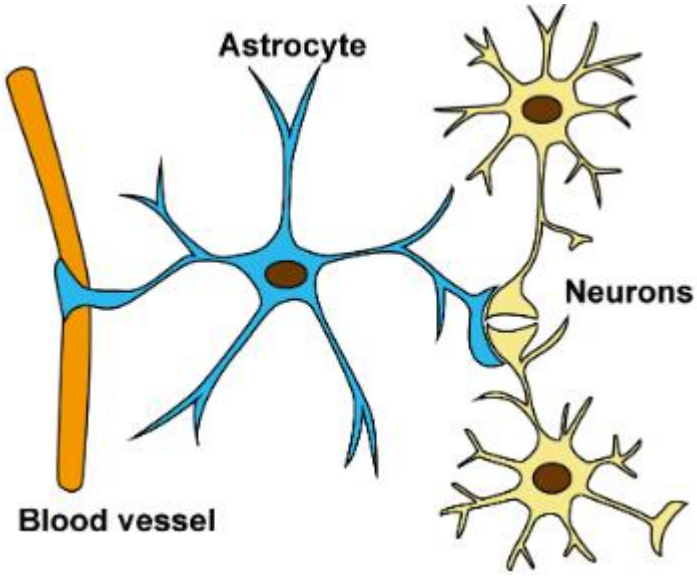

Figure 1: Anatomical composition of astrocyte connecting blood vessel and neurons in the brain [7].

Astrocytes are sensible to any insults occurred in CNS, causing a reactive response called astrogliosis. This effect has been studied to control the clinical signs of pathological changes, considering a reliable and sensitive marker for brain tissue diseases [8].

Diagnostics of TBI mostly rely on neurological examination and radiographic imaging, usually via computed tomography (CT) and magnetic resonance imaging (MRI) [9].

In general, neuroimaging methods are clinically derived with descriptive statements providing qualitative data about presence/absence of abnormalities able to identify visually (Figure 2). Aspects of TBI-related neuropathology can be explored examining damage effects in brain connectivity and neural networks. However, traditional techniques are not enough suited to cover all type of injury effects in neural cells.

a.) **b.)**

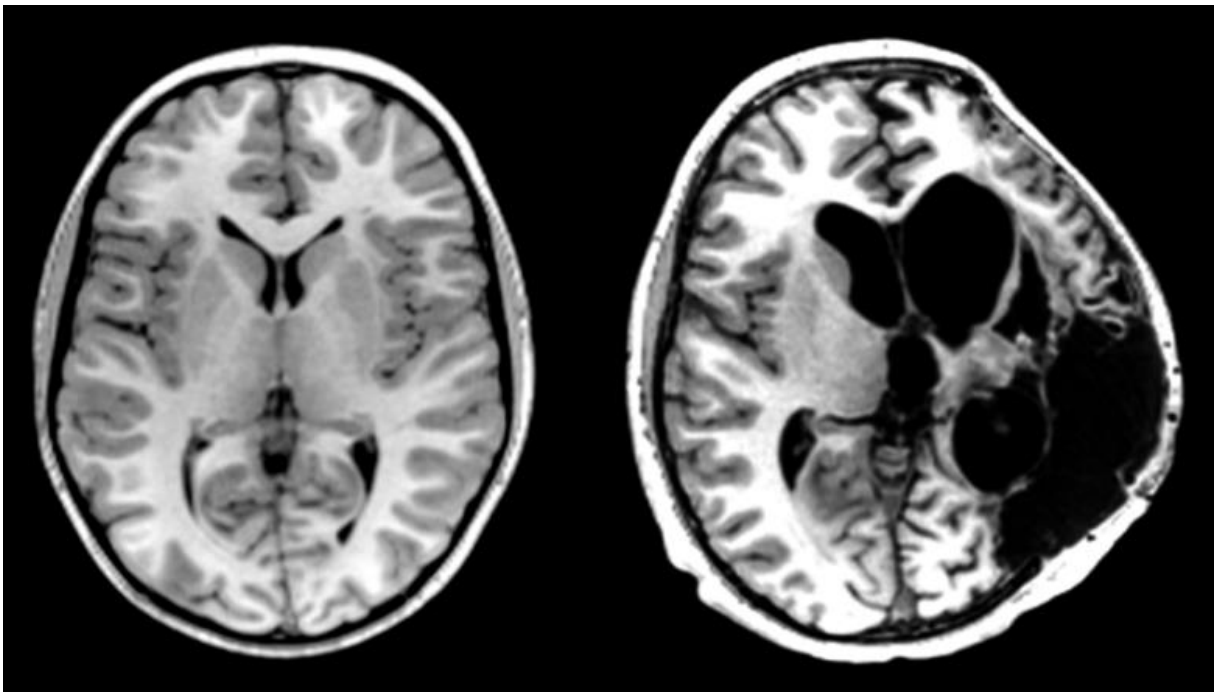

Figure 2: MR scan image used by Bigler et al. [9]. **a.)** Brain image of mild TBI with GSC = 15. **b.)** Brain image of severe TBI with GSC = 3.

Considering that, blood-based biomarkers would ease diagnosis and triage for acute treatment, clinical stratification and posterior rehabilitation for brain injured patients [10]. An ideal biomarker would provide a spectrum of TBI, involving concussion to coma, being diagnosis reference for specific treatments [11]. However, due to lack of prognostic tools, identification of specifically sensitive biomarkers to CNS biological responses is difficult [12], [13]. In recent years, potential candidates considered neuro-specific biomarkers for TBI diagnosis have been glial protein S-100β and glial fibrillary acidic protein (GFAP)[11], as a tool for glial inflammatory response analysis among others.

GFAP is an intermediate filament protein expressed by cell types in CNS including astrocytes. This protein is responsible to maintain mechanical strength of cells. The

phenomena is activated in consequence of astrocyte reactivity or damage occurred during brain injuries. Therefore, detection of elevated GFAP proteins can be used as a measure biomarker during brain damage. As well, GFAP can be detected in the peripheral blood adding benefits for TBI diagnosis [11], [14]. As well, S-100β is a specific protein of the CNS used as predictor to control neurotrophic functions that promote neurite outgrowth and proliferation of astrocytes. Protein is responsible to increase neuronal activity and functionality. Therefore, this biomarker could be interesting to control brain functionality after any trauma [15]–[17].

1.1.3 Research methods to analyse TBI

Widely varied laboratory models of TBI have been used for the investigation of brain injury mechanisms as well as for neuroprotective treatment strategies. From last century, *in vivo* [18], [19] and *in vitro* [20], [21] models have been used in an attempt to correlate mechanical insults with the resultant biological injury effects in brain. From one part, *in vivo* TBI models have shown higher biofidelity, however, complexity to perform TBI experiments in animals limits the capacity to characterize physical insults and consequential injury response. In comparison, *in vitro* models enable assessment of specific injury parameters on cellular and molecular level within a controlled environment. Performing repeatable environmentally isolated experiments, pathobiology can be monitored in real time focusing specific regions of interest. Moreover, biomechanics of injury is precisely controlled to determine effects of varied injury severities [22]. Different kind of models have been established for injury performances:

Transection

Penetrating injuries result in laceration of tissues causing localized primary axotomy and cell loss. Transection models are developed to reproduce axotomy on a macroscopic and microscopic scale [23] via plastic stylet [24], rotating scribe [25], and blades [26]. These models transect cells, causing excitotoxicity and glial activation effects [24], [27], [28]. Despite these models are scaled to perform therapeutic tests [29], primary axotomy analysis is clinically relevant for small percentage of brain injuries.

Compression

Injuries that can cause lacerations in brain tissue are mimicked with in vitro models using impactor methods [30]. Severity of trauma can be controlled adjusting the force, penetration depth, shape of the impactor and impact duration. For sliced tissue samples (acute or cultured), impactor models can generate specific regional primary injuries followed by secondary propagated effects [31]. However, characterization of injury biomechanics is limited due to difficulties to obtain a correlation between applied force and tissue deformation.

Shear strain

Shear deformation is the major causality of closed-head TBI [32], [33]. These models have been used inducing linear impact inertial loading at large shear strain rates in brain sliced cultures [34]. Measured from high-speed images, different models have been visualized by confocal microscopy to verify the cell deformation and cellular response characterization [35].

1.1.4 How to obtain cells to analyse the predictors

Focused on *in vitro* injury models, precedent studies have been employing surrogates based on the *in vivo* central nervous system (CNS), involving acute preparations, organotypic cultures, dissociates primary cultures, and immortalized cell lines. This method implies to obtain simplified surrogated samples of the *in vivo* nature. Surrogates determine the applicability being easier to use, low cost, availability and fidelity to use culturing techniques. Some limitations can be associated for developed culture systems, including lack of circulatory system and the appearance of inflammatory response of the cells. However, those characteristics may be beneficial for performances carried out under controlled conditions due to their precise addition postinjury [36].

Acute preparations

Acute preparations are explants of CNS tissue, separated and sliced (<475 μm). In general, experiments carried out using acute preparations are completed in 8 h before deteriorating begins [37]. Experimental injuries based on acute preparations have been performed on brain structures from rat frontal cortex [38], guinea pig cerebellum [39] and rat hippocampus [37]. As tissue is not dissociated, acute preparations preserve good anatomical structure, neural circulation, and

heterogeneous cell population. Moreover, extracellular matrix remains intact within its composition, bioactivity and mechanical properties. However, the effect of isolated tissue limits the response to subsequent trauma, and the *in vitro* response may be altered due to secondary diluted injury mediators.

Organotypic cultures

Organotypic cultures are obtained as thins slices of CNS tissue (250-400 μm) and maintained for extended periods (in excess of 7 days). Normally, tissue is taken from hippocampus structure due to its ability to generate slices parallel to lamellar circuitry (Figure 3).

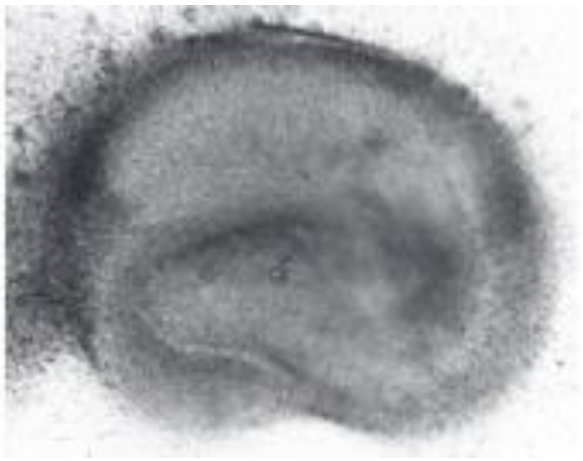

Figure 3: A bright field transmission image of an organotypic hippocampal slice culture generated from a P8 rat and cultured for 14 days [36].

Similar to acute preparations, these cultures are not dissociated, allowing specific regional analysis [40]–[42]. As well, mixed cultures can be created, including coronal brain sections [36] or thalamus and cortex [30].

Moreover, histological and morphological structure of cultures widely mimic the *in vivo* organization [19], [43], [44]. *In vitro*, synaptic and spine morphology maturing is also determined [45]. Advantage that organotypic cultures have shown is the ability to recover from trauma before experimentations. Sliding the tissue cause some damage and death of cell structure, however, recovering properties easy to obtain suitable cultures.

Dissociated primary cultures

Primary cultures are enzymatically and mechanically separated from brain tissue. For this kind, astrocytes and microglia are most suitable for culturing due to their expansion ability [20]. Neural cell cultures have been successfully modelled with astrocytes to examine mechanical injury. Also, dissociated cell cultures enable to analyse injury effects on a single cell type or in cultures where different cells are combined. However, age of cell limits the use of primary cultures. Embryonic or postnatal tissue are easy to harvest, but cellular phenotype and injury response can be significantly affected when older cells are harvested [46].

Immortalized cell lines

Immortalized cell lines easy to get, consistent, well characterized and easy to scale up for large performances. However, this process entails disruption of intracellular signalling cascades and apoptotic machinery. Consequently, contact dependency and poor adhesion are issues for injury modelling [47]–[49]

1.2 Background

The purpose of this project is to develop new strategies for TBI study. With the aim to introduce new methods for impact model approaches, similar studies have been found in the literature. These models are predecessors for fundamental understanding of cause and effect of traumatic events.

Study carried out by Bottlang et al. [34] used *in vitro* TBI models based on organotypic brain cultures. Being able to preserve the heterogeneous cell population and cytoarchitecture of brain in a controlled environment, are suitable to combine high degree of biofidelity with the ability to control mechanical insults. They developed an organotypic neural shear injury model (NSI) able to perform inertia-driven shear strain to analyse scalable mechanotrauma (Figure 4). They hypothesized that scalable deformations and resultant injury in sliced brain cell cultures can be generated within impact-induced inertial loading. NSI model was characterized correlating shear deformation of cultures to cell death.

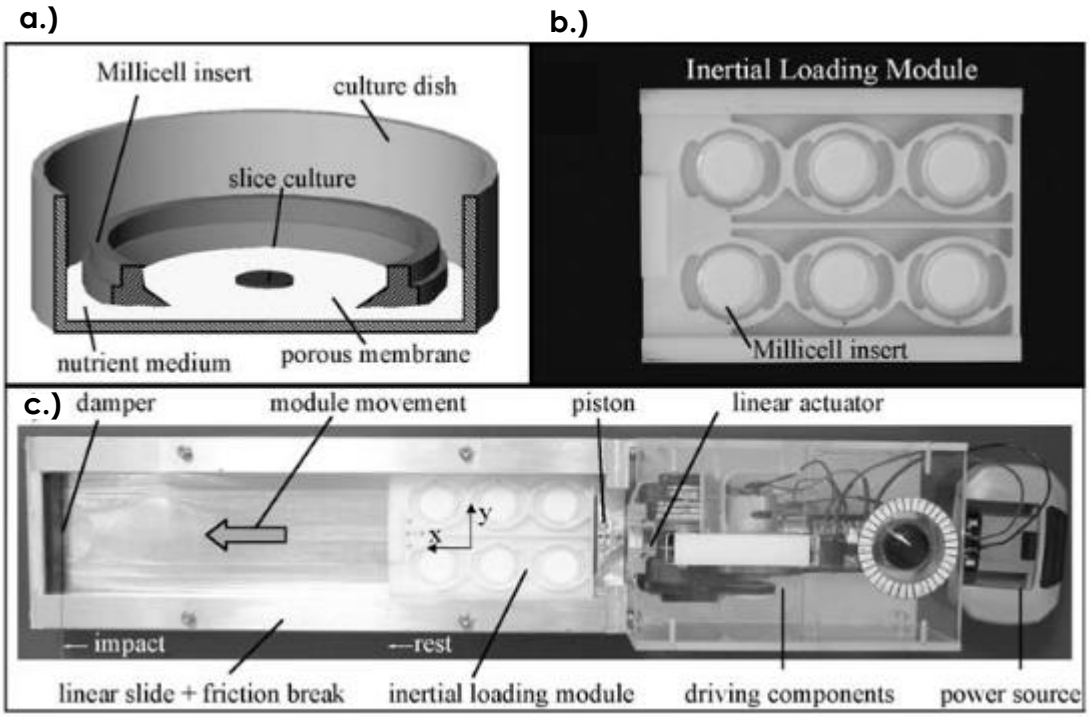

Figure 4: **a.)** Hippocampal slices as organotypic cultures on Millicell inserts. **b.)** Milicell insert sets setup for inertial loadiang module. **c.)** NSI system. [34]

Other projects involving *in vitro* TBI models elucidate mentioned mechanisms of brain injuries. Bar-Kochba et al. [50], used a 3D *in vitro* neuronal compression model, to investigate the role of impact strain and strain rate on neuronal lifetime, viability, and pathomorphology (Figure 5).

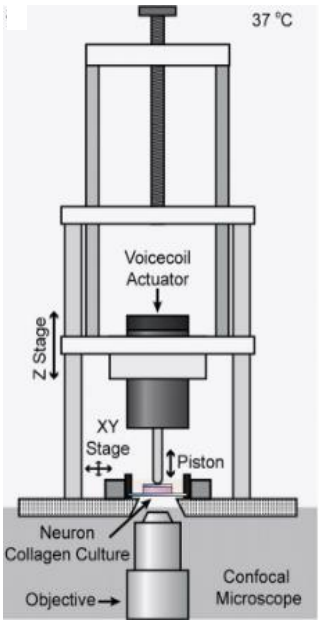

Figure 5: 3D neuronal compression device developed by Bar-Kochba et al. [50] for impact strain approaches.

Primary cortical neurons embedded in Type I collagen gels were used in different loading regimes. They found that strain magnitude result in different effects on the injury pathology. They conclude that strain magnitude affects directly on neural death time, and strain rate has more influence on the pathomorphology and population injury.

From other hand, Koumlis et al. [51], developed an *in vitro* TBI model using the Highly Automated Mechanical Impactor (HAMr). The device was designed to perform low amplitude repetitive impacts that could lead to non-diagnosed concussions (Figure 6).

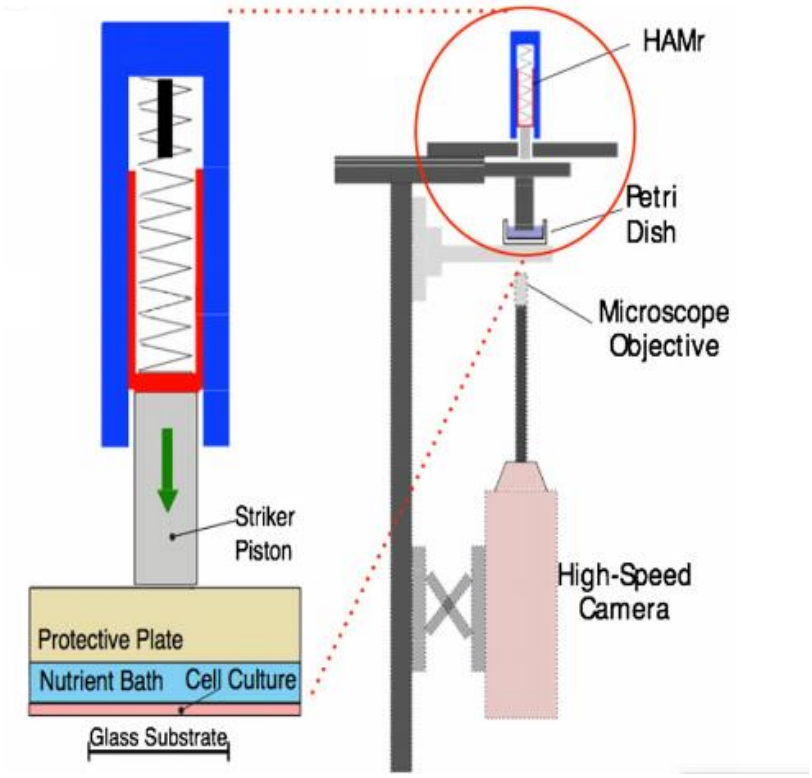

Figure 6: Schematic of HAMr device developed by Koulis et al. [51].

Leveraging potential energy of a loaded spring, a striker piston is released to perform impacts. With the aim to mimic the anatomical structure of the head, cell culture model is designed in different layers: (i) protective plate to mimic the skull, (ii) nutrient bath to mimic cerebrospinal fluid and (iii) cell culture is the brain surrogate tissue.

Cell cultures were derived from postnatal Sprague Dawley rat pups. 80% astrocytes and 20% microglia mixing were used from the cerebral cortex of rats. The study focused on to identify inflammation and damage on the glial cultures after repeated impacts. Deformation of dynamic loading was quantified in an attempt to correlate biological response to mechanical response of surrogate tissue.

To characterize and reproduce clinically meaningful mechanical insults, these new models were designed to induce repeated mechanical impacts. Working in a controlled environment, development of automated impact devices allows to reproduce experiments with mechanical and biological fidelity for TBI effect studies.

2. Motivation and objectives

The aim and motivation of this project (master thesis) is to create an embedded TBI detection system (damages localisation and acuity) based on a new multiscale biomechanical model of head impact for diagnostic and prevention. In order to estimate biological damages from impact measurements, the new system will be able to translate the macroscopic impact characteristics into biological damages for use in connected medicine to deliver high quality care on site.

The main objective of the project is to develop an impacting device for neural cells. The impact bench will be characterized by controlled and highly reproducible impact properties (acceleration peaks, contact time, etc.). In order to implement a controlled impact test on a neural cell model, accelerometers will be equipped, and primary cultures of mixed neuronal/glial cells (generated from embryonic E16 C57BL/6 mice) as well as cells from 5xFAD transgenic mouse model with Alzheimer's disease (AD) will be used for experimentation.

Secondary objective will be the cell testing after impact analysis in order to determine changes in the topology of the axons detecting Diffuse Axonal Injury (DAI). In addition, the detection of neuro-inflammation markers (GFAP, S-100-β, etc.) will be performed to leverage TBI analysis.

This way the objectives have been completed in function of the following operative tasks:

- Modelling 3D design of an impacting device and selection of materials.
- CAD of the impact device (3D Experience).
- Compute finite element modelling (FEM) for dynamical simulations.
- Manufacturing the device.
- Data acquisition of impacts and following device characterisation to verify the performance of impacts.
- Biological characterization to determine TBI factors.

The following diagram shows the procedure followed to complete the tasks.

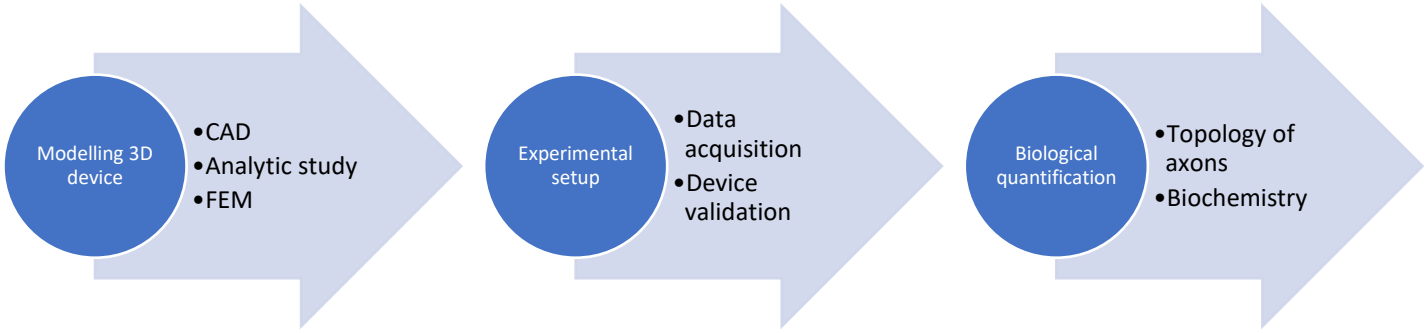

In order to follow the project efficiently and satisfy the marked objectives, a planification strategy has been established in function of determined tasks as depicted in Figure 7.

ACTUAL SCHEDULE	2021								2022			
	9		10		11		12		1		2	
	1 to 15	15 to 30	1 to 15	15 to 31	1 to 15	15 to 30	1 to 15	15 to 31	1 to 15	15 to 31	1 to 15	15 to 28
State of the art												
3D device design												
Modelling impacts and choice of material												
Impact device CAD (3D Experience)												
Compute finite element modelling (FEM) for dynamical simulations of the analytic design												
Element orders												
Manufacturing of the device												
Data acquisition of												
Device charcterisation: verify performance of impacts												
Cell testing												
Experiment schedule planning												
Biological quantification:												
Report redaction												

Figure 7: Planification strategy for project development. Completed task highlighted in green. Tasks predicted for future approaches highlighted in red.

3. Development of the project

In this section the main aspects for project developing are specified. The description of the project is included for a better understanding of the methodology followed to complete requirements of the work.

3.1 Description of the project

Quantification of diagnostic biomarkers could widely help for better diagnosis, treatment, and improvement of the outcomes for the patients. Focused on that, TBI research must be induced to find prevention, diagnosis, and future treatment approaches through fundamental understanding of TBI injury processes.

Although these new approaches widely open research in this field for future studies, there is still a scientific question to resolve. Correlation between dynamical deformations and biological effects is not systematically quantified yet. In an effort to overcome this gap, first phase of this study documents the development of a novel impact device for *in vitro* model of TBI. Developed to focus on low-energy transfer impacts, the device is prepared to test neural cell cultures in a controlled environment. In an attempt to characterize mechanical response of the impacts, acceleration forces and contact time are recorded for further studies to obtain a direct correlation with predetermined biomarkers. This way, the goal is to identify biological response in function of stablished mechanical properties.

For second phase, experiments to detect neuro-inflammation biomarkers (GFAP, S100-β, etc.) will be carried out [51], [52]. Cultured neural cells will be tested to single or repetitive impacts. Different contact time intervals and with different peak forces will be taking into account. In all cases, AI-based High Content Screening (HCS) microscopy will be used to obtain an unbiased comprehensive immunocytochemical and morphological assessment of thousands of cells on the post-impact dynamics of: (i) neuronal viability (βIII-tubulin, MAP-2, caspase 3, MTT test) (ii) synaptic integrity (PSD95, synaptophysin); and (iii) glial inflammatory response (GFAP, S-100β, Iba1). Quantitative biochemical measures of prototypic pro-inflammatory cytokines and

AD-linked beta amyloid peptide (Aβ40 and Aβ42) will be performed by ELISA MSD on cell supernatants.

3.2 Design strategy

The design strategy involves all methodology procedures performed to develop the impact device. Characteristics of the device and its elements are described including design and manufacturing procedures. As well, performed analytical, computational, and experimental approaches are specified.

3.2.1 Device development

Shock cell device has been designed to work to receive impacts in vertical orientation. The aim of the device configuration is to reproduce experiments subject to inertia and gravity itself.

The device has been developed to be strong enough to support repeated impacts. Stainless steel material has been opted for main base of the structure to enable a solid support during vibrations as well as for parts which interacts in those impacts. Initially, those elements have been manufactured via waterjet cutting method obtaining basic structures to ease the following machining processes. In combination, aluminium material has been used for vertical beam and other smaller parts with the aim to reduce the weight of the whole device.

The device consists of five main components: guided sliding table, versatile working plate, bumper, height positioner, and the brake system (Figure 8).

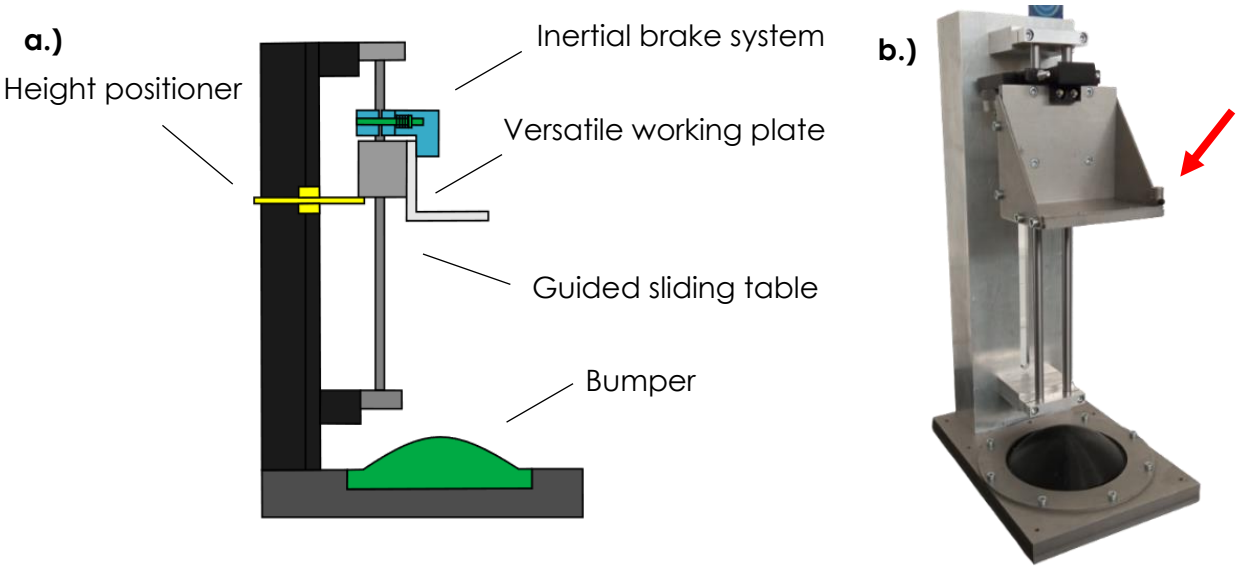

Figure 8: Shock cell device. **a.)** Side section view of the full mounted device. **b.)** Manufactured real device. Pointed by red arrow, the accelerometer fixed in the versatile working plate.

The guided sliding table is a commercially available sliding system (available at ECMU). A moving table centred within the pillars is integrated with roller ball bearings, avoiding high friction restrictions.

Fixed to the moving table, the versatile working plate is attached. The plate has been designed to be able to fix different kind of cell culture petri dishes as well as accelerometers for data acquisition during experiments. For that, the working space has been machined with several fix-points (threaded holes). Furthermore, this supposes a reduction of the weight of all moving part. Considering it is subjected directly to impacts, lateral reinforcements have been added to reduce non desired reactions and vibrations.

Positioned in the low part of the device, the bumper is centred within the versatile working space. The impact occurs between the lowest part of the versatile working space and the highest point of the bumper. In order to avoid non desired vibrations during the impact, bumper is centred with the centre of gravity of the plate and tightened with a stainless-steel collier. This way, it is possible to ensure that the main impact is going to be concentrated in a determined region (where cell culture petri dishes are placed).

The bumpers have been manufactured via 3D printing. In this project, fused filament fabrication (FFF) technique has been used with the Volumic stream30 dual MK2 printer. Thermoplastic polyurethane (TPU) (Ninja Flex93 Ultra) has been used obtaining bumpers with E = 5-30 MPa. Four different bumpers have been manufactured with R = 50 mm, 100 mm, 300 mm and 1000 mm.

Experiments have been performed varying the maximum acceleration and contact time during the impact. Based on information obtained from previous studies involving mild TBI, prominent range values for acceleration and contact time are estimated. Combining the Young's modulus of the material (E) and the radius of curvature of the geometry (R) it is possible to adapt the bumper dimensioning to match with those estimated acceleration and contact time values. This way, it has been possible to identify needed properties to ensure a coherent working setup.

The resultant maximum acceleration and contact time is also given in function of the impact velocity. Following equation (1), velocity is given in function of the height position.

$$u_0 = \sqrt{2gh} \tag{1}$$

For that, a manual height positioner has been included. The system consists in a simple steel bar capable to fix in different specific height along the vertical beam. The moving table is placed in the bar determining the initial position for each experiment. Considering the beam height, five different positions have been determined from 10 to 30 cm, obtaining a range of velocities between 1 m/s and 3 m/s.

Regarding nature of experiments, it is expected to obtain most essential information with the very first contact. For that, an inertial braking system has been included to stop the movement of the plate after the first impact. That way, it is possible to avoid posterior impacts which results basically in non-desired vibrations captured as noisy data. The brake system works leveraging the potential energy of springs confronted with the guided sliding system pillars. Once the springs are loaded, weighted parts are placed between surfaces where pillars are situated, creating a gap which enables the free movement of the plate. To ease the colocation of the weights, a pushing part is included to force the springs. When the impact occurs, due to inertia, weighted parts are discharged allowing the springs to clamp the pillars stopping the system. All parts of the system have been manufactured via 3D printing techniques (Figure 9).

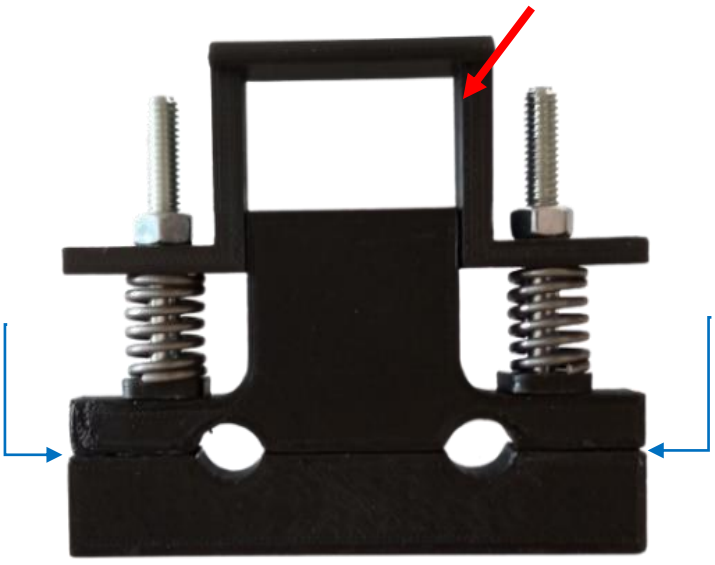

Figure 9: Inertial braking system. In function of how much the springs are tightened, the friction increases against the pillars in the guided sliding system. Pointed by red arrow, the pushing part is included to ease the movement of springs. Pointed by blue arrows, the gap is created between the surfaces to insert the weighted parts and create the gap against the pillars centred in the holes.

Regarding manufactured elements, the models have been developed with 3D experience platform and Solidworks software. At the same time, it is possible to make different kind of assemblies to verify all parts combine and fix perfectly before any manufacturing process. With that, all CAD files have been created (attached in annexes) to ease the understanding of each element of the device. Furthermore, it is possible to reproduce future models in order to perform computational simulations (for numerical studies) based on obtained assemblies.

3.2.2 Bumper dimensioning

The main objective is to perform extensive testing of neural cells to impacts. The first step is to design a reliable impact apparatus to perform reproducible impacts in terms of contact time and maximal accelerations. Contact time, T_c and maximal acceleration, $\ddot{\delta}$, of an impact vary with impact velocity u_0 and the mechanical design of the bumper. The bumper being the target contact surface, a preliminary analysis has been carried out to determine its mechanical and geometrical specifications before its manufacturing. Bumper dimensioning consisted in determining the range of interesting curvature radius R of the contact region and young modulus E of the material. Combinations of both characteristics specify different bumpers. For a fixed impact velocity, different geometries and mechanical properties, allowed to change exposure time (contact time during the impact) and maximal inertial forces.

A quasi-static modelling of impact based on Hertz contact has been built to determine contact time and maximal acceleration. This model is based on a Hertz contact force, a massive bumper and a rigid impactor. We obtain the penetration depth (δ_{max}), contact time and acceleration,

$$\delta_{max} = \left(\frac{5}{4}\frac{m{u_0}^2}{E\sqrt{R}}\right)^{2/5} \quad (2)$$

$$T_c = \frac{1}{\alpha}\left(\frac{m}{E\sqrt{Ru_0}}\right)^{2/5} \quad (3)$$

$$|\ddot{\delta}| = \frac{1}{\beta}\frac{E\sqrt{R\delta^{3/2}}}{m} \quad (4)$$

Where, m is the mass of the part which will contact the bumper with a velocity u_0, E the young's modulus of the bumper and R its radius of curvature. Note that equation 3 and 4 are scaling laws where prefactors α and β are missing.

This simple modelling enables to estimate different range of values for acceleration and contact time. Based on mechanical impact approaches found in literature, the analysis has been carried out in the physiological range of 20 – 200 m/s² for acceleration and 2 - 7 ms for contact time [53]. Combination of different radius of curvature (50 to 1000 mm) and Young's modulus (1 to 1000 MPa) have been considered to achieve acceleration and contact times. The analysis has been developed using Matlab software. This method ensures to identify which of the combination of determined properties (E and R) match with acceleration and contact time stablished for mild TBI.

Acc(m/s²) / TC (ms)	20	50	75	100	125	150	200
2							
3							
4							
5					E = 30 Mpa R= 1000 mm	E = 30 Mpa R= 1000 mm	E = 30 Mpa R= 1000 mm
6			E = 30 Mpa R= 1000 mm	E = 30 Mpa R= 300 mm	E = 30 Mpa R= 300 mm	E = 100 Mpa R= 50 mm	
7				E = 30 Mpa R= 300 mm	E = 30 Mpa R= 300 mm		

Figure 10: Bumper case characterization. Based on determined acceleration and contact time, match cases have been identified finding optimum properties for bumper dimensioning. Three different bumpers, combining E = 30 MPa and 100 MPa, and R = 50 mm, 300 mm and 1000 mm.

As depicted in Figure 10, three bumpers have been identified in function of E and R: E = 30 MPa and R = 300 mm and 1000 mm; E = 100 MPa and R = 50 mm. The code has been improved to select unique cases matching Tc and $\ddot{\delta}$ for the set of bumpers. This way, repeated cases are removed. In addition, a bumper with R = 100 mm has been added to widening the range of study for this project.

3.3 Modelling

3.3.1 Analytic study

As mentioned, an analytic study has been performed to determine the basics of the impact model behaviour. The analysis has been performed based on characteristics determined for device design and bumper dimensioning. In function of the velocity impacts (related with initial height position) and properties of different bumper cases, it has been possible to predict the behaviour of the device. Based on theoretical hypothesis, Hertz impact model equations have been used for data interpretation. Considering scaling law equations of the modelling, analytical performance has been used to stablish the reference model for the device behaviour. The study has been carried out with Matlab software being able to obtain interpretative data for further analysis. Leveraging the code, determined prefactors have been found from acquired data to stablish the primary functionality threshold. This way, assuming primary theoretical behaviour of the device, it has been possible to compare computational and experimental analysis with estimated analytical workability.

3.3.2 Computational study

Computational simulations have been performed via the 3D Experience platform. Structural model creation app has been used to prepare the model (mesh, connections and material). Then, simulations have been performed with the mechanical scenario creation app. In order to ease computational tasks, a simplified model have been used, analysing only the critical contact regions. In this simulations, selected parts are the versatile working plate and the bumper as depicted in Figure 11.

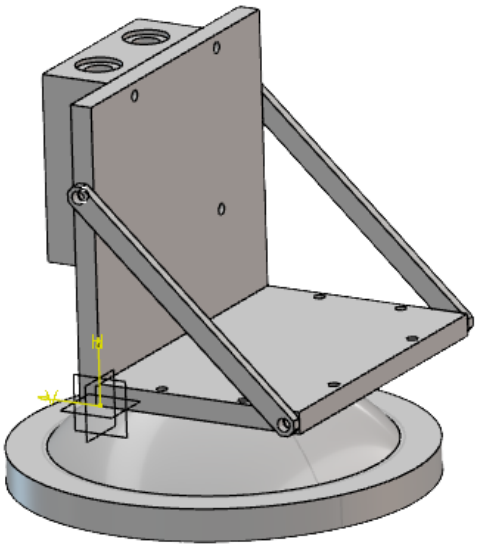

Figure 11: Simplified model for computational analysis. The model includes only relevant elements. The versatile working plate fixed with the sliding table and the selected bumper with radius of 100 mm.

Structural model creation

The impact apparatus has been designed in 3D within the structural model creation app. Virtual connections such as virtual bolts and fixed elements have been established in regions where different parts must be fixed.

In order to complete simulations as real as possible, stainless-steel has been applied to the versatile working plate and a rubber for the bumper. Properties such as density of the material, Young's modulus and Poisson's ratio have been stablished for each case. Stainless-steel has been configured with a density of 7500 kg/m³, E = 190 GPa and Poisson's ratio of 0,265. The rubber material has been applied with a density of 950 kg/m³, a Poisson's ratio of 0,49 and different Young's modulus being 30 MPa, 100 MPa, 300 MPa and 1000 MPa. Note that values for E obtained from analytical study does not include 300 MPa and 1000 MPa. In order to widening the range of study, those simulations have been included as well.

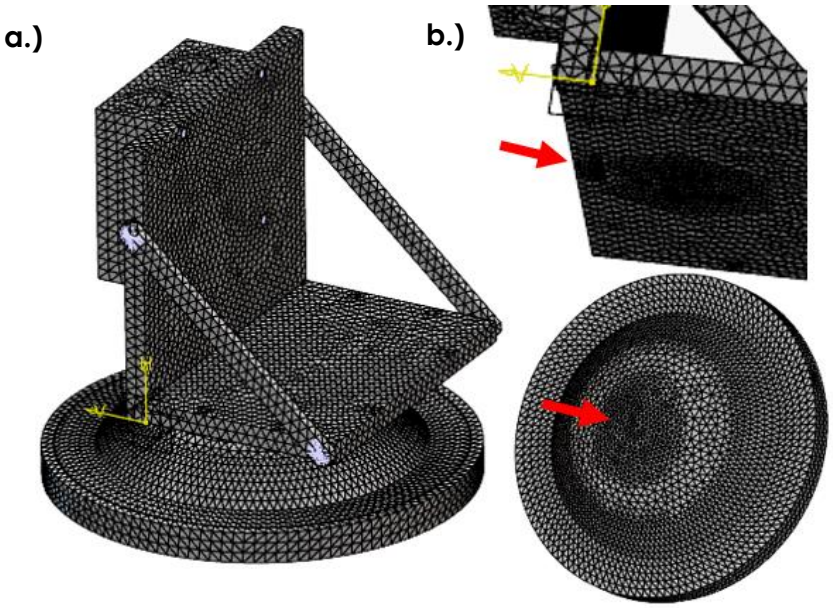

Figure 12: Meshing of the simulation model. **a.)** Loosely meshed model. **b.)** Red arrow: refined meshing at the contact region (bottom of the versatile working plate). **c.)** Red arrow: refined meshing at contact region (highest part of the bumper).

Otherwise, a required mesh has been applied for computational analysis. Regarding the mesh, it has been decided to create a loose mesh as generic for all parts, and a refined mesh for regions and/or surfaces where contact is likely to occur (Figure 12). In any case, tetrahedral meshing has been applied.

A very refined mesh enables accurate results, but requires high computational cost, resulting in time-consuming simulations. Therefore, a preliminary convergence analysis has been done in order to obtain best equilibrium between good mesh quality and computational time (less than 5% difference when refining mesh dimension by 2).

As shown in Table 4, three combinations have been selected combining general and regional surface refined meshes in such order: 10 - 5 mm, 5 - 3 mm and 1.5 - 3 mm.

	Element	Nforce (N)	$\ddot{\delta}$ (m/s²)	Tc (ms)
Mesh1: 10-5 mm	Bumper	2028	[redacted]	10
	Moving part	1950	459	
Mesh2: 5-3 mm	Bumper	1670.5	[redacted]	13
	Moving part	1904.3	374	
Mesh3: 1.5-3 mm	Bumper	1673.5	[redacted]	13
	Moving part	1817.8	373.6	

Table 4: Convergence analysis performed for mesh selection. Coloured in green, selected mesh with a general meshing of 5 mm and a refined regional meshing of 3 mm.

The convergence analysis has been carried out involving three properties: Reaction forces (focused mostly on reactions in vertical direction) in the contact region (Nforce) given in Newtons (N), maximal acceleration and contact time. Regarding obtained results, for first sight mesh 1 has been neglected. Mesh 2 and mesh 3 show almost no variation for reaction forces and contact time. However, computation time differs from tens of minutes (Mesh 2) to days (Mesh 3). Considering the rest of our analysis, we selected mesh 2.

Mechanical scenario creation

Simulations have been computed via mechanical scenario creation app of 3D Experience software. In order to compute contact-based simulations, it is necessary to determine some boundary and initial conditions to prepare the simulation scenario:

The procedure of the simulations has been performed using implicit dynamic steps which configures stress/displacement analysis. Initial velocities from 1 to 6 m/s have been applied to the moving part to simulate different cases encountered in the experiment. For specific interactions, surface-based contact condition is applied to ensure which surfaces are in contact (in this case, the bumper and the versatile working plate). Apart from that, in order to restrain undesired displacements bumper has been clamped and moving part is restricted to move only in direction z. In addition, gravity is applied as an external force to the moving part. To ease the computational time, the gap (vertical distance) between versatile working plate and the bumper has been minimized and determined to be the same for every simulation case (1 mm). This enables to start the contact in the very first steps.

Estimated values for contact time obtained from the analytical procedure have been considered to configure simulation timestep (time stablished for each increment) and duration. The timestep is estimated from the following equation (6). This value is determined in function of maximum increments which has been determined to be 200 steps. The duration of the simulation has been determined to be twice the contact time obtained from analytic values (Equation 7).

$$Timestep = \frac{2 \cdot T_c}{200} \tag{6}$$

$$Duration = 2 \cdot T_c \tag{7}$$

Being T_c contact time obtained from analytic scaling law. As each independent case shows different initial values, timestep and duration must be configured for each simulation.

24 cases have been computed with four Young's modulus (E = 1000 MPa, 300 MPa, 100 MPa and 30 MPa) and six velocities (1 to 6 m/s). Considering computational time and capacity, it has been decided to perform the simulations with only one bumper. In this case, the simulations have been carried out with a single radius of curvature R = 100 mm.

From the simulations, maximal acceleration, contact time and reaction forces in the contact region have been acquired. Apart from that, contact pressure has been analysed as well. As depicted in Figure 13, it is possible to check the deformation effect of the contact pressure during the impact.

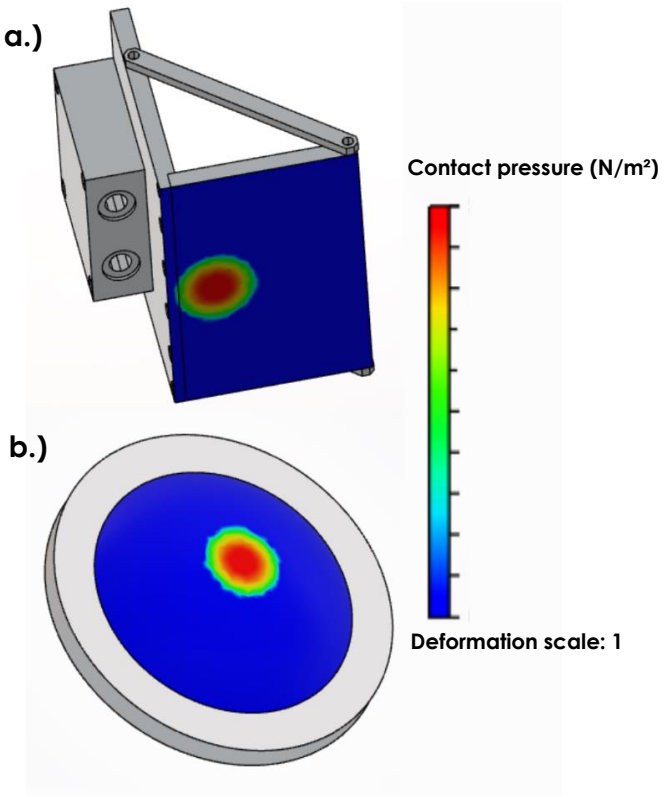

Figure 13: Resultant contact pressure analysed during computational simulations within impact velocity of 6 m/s. Acquired values show contact pressure at maximum acceleration, at ≈ 0,85 ms after contact begins. **a.)** Contact pressure pattern in the versatile working plate. **b.)** Contact pressure pattern in the bumper (R=100, E=300MPa.

The simulation model shows the distribution of the impact along the contact region, spreading the resultant pressure uniformly in both surfaces (lowest part of versatile working plate and highest part of the bumper). Measured in N/m², and deformation scale being 1 (values are scaled by 1) values show symmetrically how the highest forces are centred in main contact part (being augmented during impact period) and it is transferred over the surfaces. At the same time, regions that are not receiving any contact remains without any resultant deformations. This confirms that most of the impact is going to produce in the centred contact region.

3.4 Experimental setup

3.4.1 Data acquisition system

Data is acquired from a precision accelerometer (A/120/V 10, DJB Instruments) screwed on top of the versatile working plate. The accelerometer signal is produced with an IEPE signal conditioner (VB/01, DJB Instruments). The signal is recorded with a high frequency data acquisition system (U3-HV, LabJack). The electronic system is connected to a micro-computer (Raspberry-pi 4 model B, Raspberry-pi foundation) which enables to create the automated acquisition system using Python.

The data acquisition code is integrated with a Node-Red interface enabling to record data in real time for each experiment. To ease data acquisition, a user-friendly dashboard (Figure 14) allows to set recording properties (sample frequency, experiment duration, csv file and folder names) and fast processing properties (acceleration threshold). The impact acceleration signal is plotted directly on the dashboard for fast validation of the test. All experiments are saved on the computer for further data treatment.

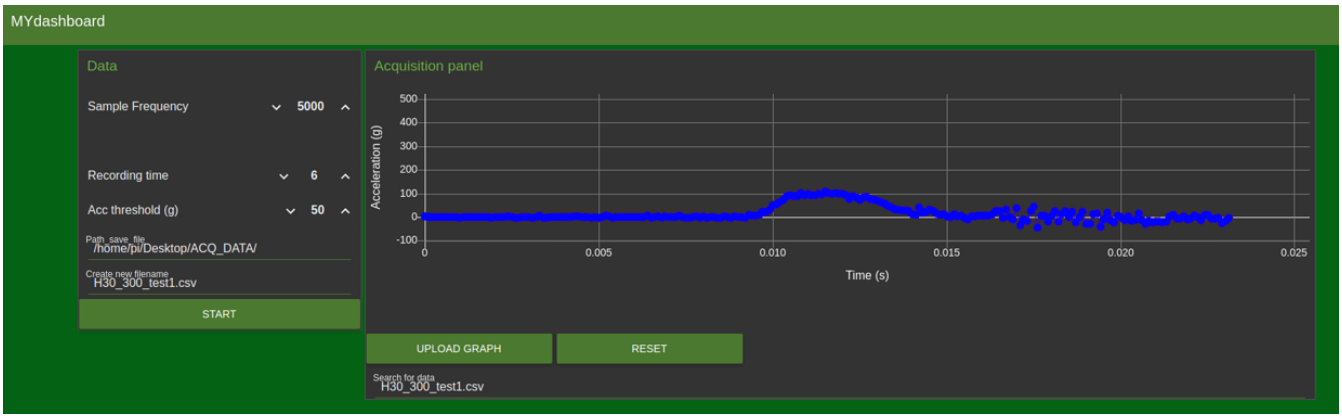

Figure 14: User-friendly dashboard integrated by nodered platform. Data acquisition and saving is automated easing the experiments performance. This dashboard shows one experiment performed with impact velocity of 2.4 m/s (h = 30 cm) and bumper of R = 300 mm and E = 5 MPa.

3.4.2 Data treatment

Raw data is recorded with a high sampling frequency (4-10 kHz). Large files of data points are produced. Sensor noise is in the order of 5g with extremely high frequency content. Data cleaning is applied with a Matlab code, by filtering high frequency content (moving mean filter) and selecting the desired frame around the impact instant as depicted in Figure 15. The magnitude of the acceleration at the

impact and the impact duration are the outputs of the data treatment. Results are not affected by the chosen thresholds and filters.

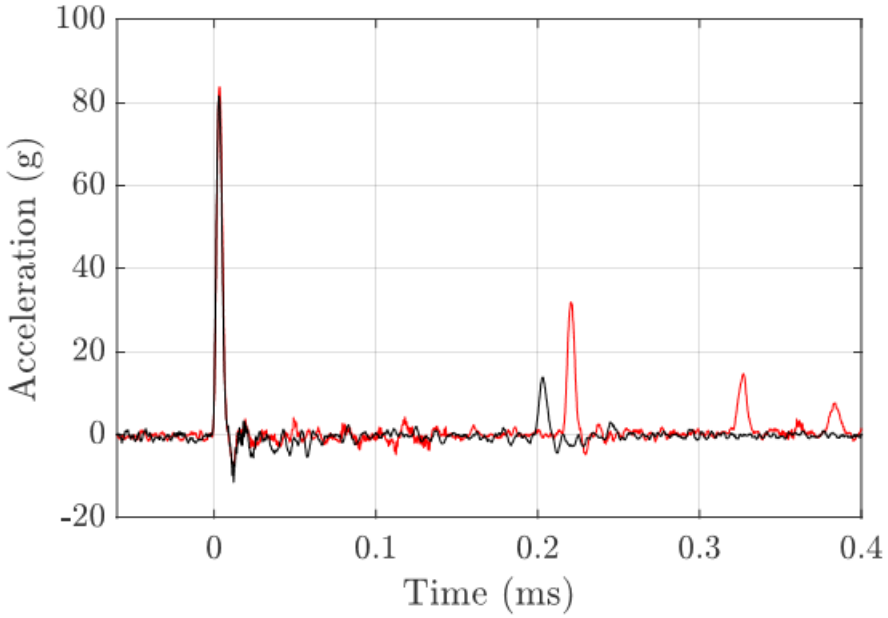

Figure 15: Processed acquired data signals. Black signal shows data acquired including the inertial braking system. Red signal is acquired without the braking system. The graphic shows the effect of the braking system reducing posterior non desired impacts as well as acquisition of les noisy data.

3.4.3 Experimental test performance

In order to validate the impact device, an experimental approach has been performed. The impactor has been tested in primary conditions (no data acquisition) to verify its workability and functionality after manufacturing and mounting. The aim of first validation is to check the behaviour of the main components against impacts and produced vibrations. From one part, the inertial braking system has been proved. Under same conditions (same bumper and impact velocity), the experiments have been carried out with and without the braking system. As depicted in Figure 15 it is possible to check the effect of the braking system in the resultant signal. When the brake is not included, within minimal friction in the sliding table the versatile working plate continues bouncing showing several impacts. As a result, acquired data records non desired acceleration peaks as well as much more noise due to vibrations. In contrary, when the braking system is integrated, after first impact the system is clamped. This avoids posterior non desired impacts and vibrations. Note that depending on the impact velocity, it is possible to obtain a second lower impact

which determines that the system is not totally stopped. However, acquired data is cleaner.

In conclusion, data shows that regarding desired impact (very first contact) the braking system hardly affects in the results, obtaining same values. Considering the goal of the inertial braking system is to avoid non desired posterior impacts and vibrations (noise), the functionality of the same has been proved.

Once the inertial braking system is validated, the calibration of the data acquisition system has been carried out. As mentioned, vibrations occurred during impacts will be recorded affecting resultant signal. For that, accelerometer fixed in the versatile working plate has been tested to ensure acquired data is coherent. This will ease the understanding of the acquired data, enabling to set required thresholds to avoid non desired noise.

Secondly, the versatile working plate has been tested with all different bumper and determined impact velocities (testing at different height). To validate the data acquisition as well as device functionality at the same time, different tests have been performed.

With the system calibrated, required experiments have been carried out. With the same criteria, data has been acquired performing different tests involving all the bumpers at all predetermined impact velocities. In order to obtain more robust results, each bumper has been tested seven times per impact velocity. Therefore, 35 different tests have been performed for each bumper (5 impact velocities times 7 tests), resulting in 150 tests in total (35 tests times 4 bumpers).

4. Results

4.1 Device results

In general, manufacturing process have been followed as predicted. Leveraging previously machined parts (by external company using waterjet cutting techniques), finishing steps have been eased. However, based on the results seen in the manufacturing phase, it has been necessary to overcome some characteristics of the first design.

At first sight, dimensioning has been done as an estimation in an attempt to manufacture a device as compact as possible. Moreover, taking into account commercial elements, the design has been adapted to fix all elements correctly. This supposed to maintain a continuous control to ensure all manufactured elements were machined properly. For that part, lack of resources and difficulties seen to machine precisely all the aspects of some parts (due to used stainless-steel materials), processes took more time than expected. Fixing all characteristics such as positioning of threaded holes (necessary to be checked every time within commercial parts) has been more thought work than estimated.

Apart from that, only redesigned element has been the structure of the versatile working plate. Considering the element which support most vibrations during the impacts, lateral guide supports included in both sides have been replaced by triangle shaped metal sheets. This way, any non-desired resultant movements (produced by the torque after impact) are reduced obtaining more stable working space.

In conclusion, besides all controls and steps followed to develop the final design of the impact device, performed experiments concluded the functionality of the same and its workability has been validated.

4.2 Raw data results

For a first comprehension and understanding of the performed experiments, acquired data (maximum acceleration and contact time) have been analysed to check the coherence regarding what theoretically is expected. Considering all cases, mean values for maximum acceleration and contact time have been recorded for

each bumper. Mean values have been obtained from repeated test in function of each impact velocity performing more robust results. As depicted in Figure 16, acquired data have been graphited comparing maximum acceleration as well as contact time for specific impact velocity and each bumper.

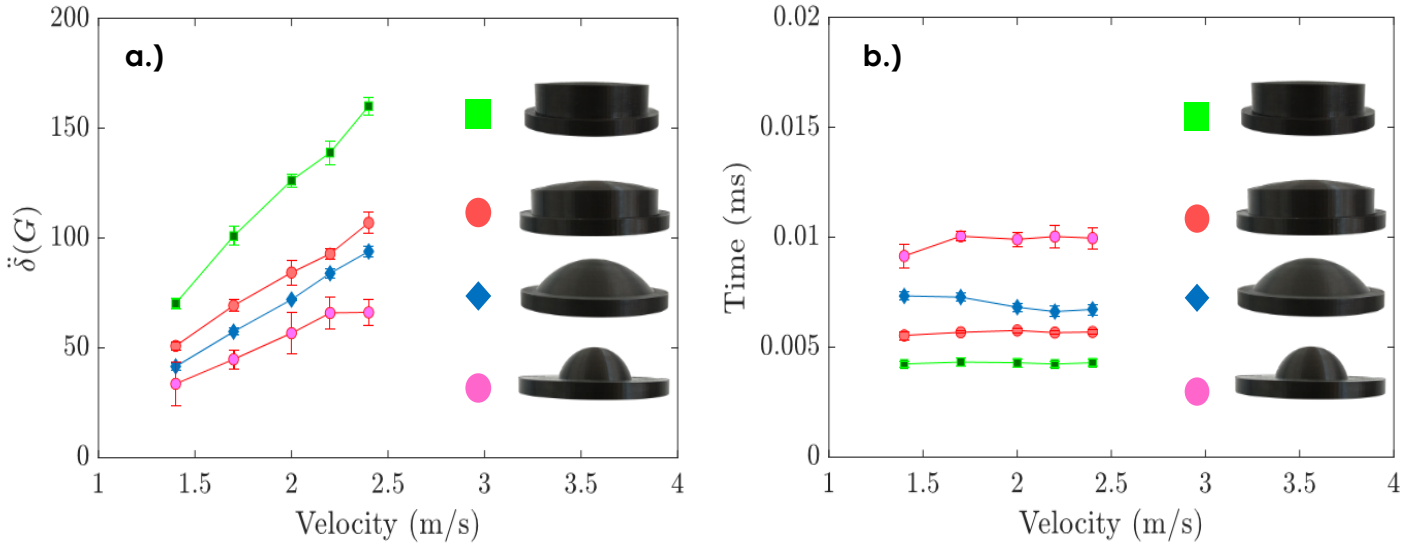

Figure 16: Dimensional raw data acquired from performed experiments. Data is compared from required four different bumper cases with same Young's modulus (E = 5 MPa). Green R = 1000 mm, red R = 300 mm, blue R = 100 mm and pink R = 50 mm. **a.)** Mean values for maximum acceleration in G in function of determined impact velocities. **b.)** Mean values for contact time in ms in function of determined impact velocities

Based on the theory, with a larger radius of curvature the contact surface increases resulting in higher acceleration peaks (Equation 4). This supposes that penetration depth during the impact is lower and in consequence the contact time decreases. In contrary, with smaller radius of curvature, contact region is sharpened enabling more deformation during the impacts. This result in higher penetration between surfaces and the contact time of the impact increases (Equation 2). At the same time, it is estimated that for higher impact velocities, resultant maximum acceleration should be increased. However, regarding contact time, for higher impact velocities opposite reaction is expected (Equation 3).

Considering obtained results, regarding acceleration the theory is confirmed. For each case, when radius of curvature of the bumper is increased, the resultant maximum acceleration is higher for each determined impact velocity. At the same time, when impact velocity is increased, the resultant acceleration increases also.

Focused on contact time, it is possible to check that when radius of curvature increases, the contact time for the impact decreases. However, when impact velocity is higher some discrepancies can be seen. Following the theory, contact time should be decreasing for every case, but it is possible to check that only bumper with R = 100 mm follow this pattern. This could be a consequence of the bumpers' material and manufacturing properties. Despite all the experiments have been carried out with same criteria, each bumper can show different behaviour. It is not possible to ensure that Young's modulus of each bumper is exactly the same as well as manufacturing process issues can change the functionality of the same. Therefore, assuming the same properties for every bumper, based on used equations and data processing codes results may not match as expected.

4.3 Global results

With the aim to analyse acquired data in a single plot (analytic, computational, and experimental), a dimensionless scaling was applied for maximal acceleration and contact time,

$$\ddot{\delta}_{scaled} = \frac{\ddot{\delta}}{\left(\frac{ER^2 g^{3/2}}{m}\right)^{2/5}} \tag{8}$$

$$TC_{scaled} = \frac{T_c}{\left(\frac{m^4}{gR^3E^4}\right)^{1/10}} \tag{9}$$

This way, data acquired from simulations and experimental phase can be compared against prefactor threshold to check the affinity regarding theoretical, computational and real results. As depicted in Figure 17, data for maximum acceleration and contact time have been graphited, both against determined height (related with impact velocity). Regarding maximum acceleration, obtained results get close to threshold determined from analytical study. This supposes that impact device is working as estimated given accurate data for further performances. Considering requirements established for computational analysis and experimental phase have

been different, getting really close results ensures estimated models and manufactured device match correctly with criteria determined from the very first hypothesized case for this project. Therefore, it is possible to confirm the functionality of Hertz impact models.

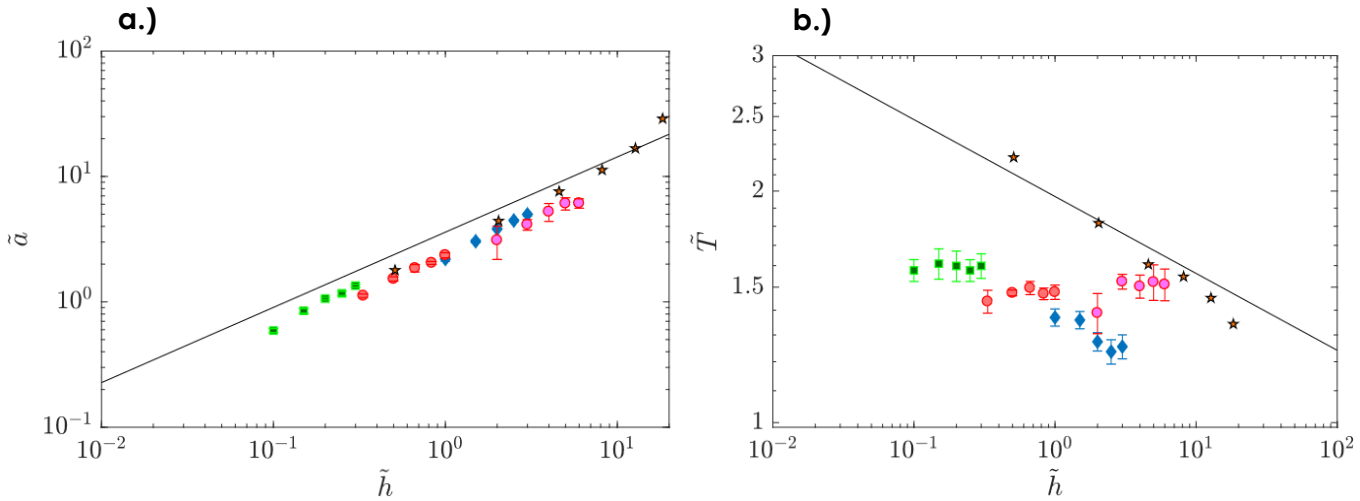

Figure 17: Non dimensional data including analytic model (threshold line), computational, and experimental values. **a.)** Maximum acceleration in function of height given by each bumper case and simulation. **b.)** Contact time in function of height given by each bumper case and simulation. Green R = 1000 mm, red R = 300 mm, blue R = 100 mm, and pink R = 50 mm. Star: computational data performed for E = 30 MPa and impact velocity from 1 to 6 m/s.

From another part, results depicted for contact time show bigger gap comparing to analytical threshold. As it has been seen with raw data depicted in Figure 7, discrepancies may come due to behaviour of the bumpers. Being difficult to control the nature of the material properties and characteristics in real experiments, it is not possible to ensure a good match with analytic and simulation results. However, regarding data acquired from computational approaches, it is possible to check that data fits accurately with analytical model. Therefore, despite some discrepancies, it is assumed that general results are compatible and coherent with performed models.

5. Conclusions

We have presented and evaluated the functionality of a novel shock cell impact device designed for experimental approaches focused on testing dynamical impacts on neural cells. Based on predecessor studies involving TBI models [50], [51], the design of the device has been adapted with the aim to be able to transfer impact effects directly to cell cultures. The device has been designed and developed to be easy to manipulate, enabling the user facilities to mount or transport the whole structure. The compact design is thought to permit a rapid manipulation of the setup, enabling to change the height positions as well as the bumpers for each experiment. As well, the high reproducibility allows to perform new tests as much as needed.

As mentioned, the manufacturing of the device has been carried out as predicted. Following main design, every part regarding stainless-steel and aluminum material has been machined fixing commercial parts to develop whole functional structure. Despite a meticulous control has been necessary to fix every element precisely, further experimental and calibration tests validated the functionality of the device.

At the same time, bumpers and smaller parts such as the inertial braking system have been manufactured with 3D printing techniques. Although this technique allows to manufacture different geometries easily and with lower cost, limited capacity of the machine increases the manufacturing time. As an example, manufacturing time for each bumper lasts one day, being impossible to produce more elements in that period. For that, several days have been occupied just to verify the quality of the bumpers as well as to produce and validate the parts for the inertial braking system.

The inertial braking system has been tested to confirm the effects on performed impacts. Depicted in Figure 15, obtained results confirm that using a braking system, acquired signal show cleaner data and produced noise due to vibrations is reduced easing data treatment.

One of the objectives proposed to this project has been to adapt the data acquisition to be totally automated. With that aim, configured data acquisition system enables to save every tested experiment automatically in a determined folder. This facilitates the collection of data for further analysis and data processing. We have seen that

sometimes, due to lack of connections, data acquisition is not well recorded. Despite of that, leveraging the high reproducibility of the device, it is possible to retake each specific experiment in case that recording has failed.

In order to check the coherence of the experimental approaches, analytical and computational analysis have been performed previously. Based on Hertz impact models, scaling law equations have been used to determine the basis of the impact testing behavior and simulations with 3D Experience platform have been carried out to estimate the results of the predetermined models. Focusing on that, due to computational capacity, it has been necessary to simplify the simulation modeling as well as to perform convergence analysis (for meshing) to ease the simulations approaches. Apart from that, results obtained show a good relation between analytical, computational and experimental data.

In conclusion, it has been possible to manufacture a totally functional impact device, being easy to manipulate and with high reproducibility capacity. Moreover, included automated data acquisition system enables to record every data for each experiment being able to save all information rapidly. Performed analytical, computational and experimental approaches show high correlation between obtained data, concluding that for now, the shock cell device is validated to perform future experiments involving cell cultures for further studies.

6. Future lines

Developed device has been tested to analyse mechanical properties in experiments using different bumper of determined material (E = 5 MPa). For future experiments, it is expected to manufacture new bumpers with different Young's modulus. For now, bumpers with E = 100 MPa are being manufactured using nylon.

Otherwise, one of the objectives proposed for the project has been to perform the biological characterisation. Once the impact device is validated, the following approach is the experimental phase for testing neural cell cultures.

The experiments will start on April in the University Hospital of Timone in Marseille. The experiments will be performed in the laboratories of the Institute of NeuroPathophysiology (INP-CNRS/AMU). The manufactured device will be moved on to the TIMONE's laboratories at the beginning of the experimental phase and will be preserved in a specific space for proper working environment. All the elements for device disposition and set up will be provided by our team, this includes all the mounting elements, tools, replacement parts, electronic devices, etc. In combination, all biological elements needed for cell culture development and preservation will be provided by neuropathophysiology team in the hospital.

Quantitative and qualitative measurements will be carried out for biologic characterization based on predetermined neural biomarkers. As mentioned in the project description, AI-based High Content Screening (HCS) microscopy will be used for immunocytochemical, and morphological characterization and ELISA tests will be performed for quantitative biochemical measurements. Image processing (shape of axons by HCS) and treatment of biological data (neuronal viability, synaptic integrity, glial inflammatory response, etc.) will be carried out. Semi-automated experiments for large scale data acquisition will provide information to perform statistical analysis between impact properties and biological effects.

It is expected to create an open database with obtained results to provide new correlated information about cellular response regarding predetermined impact procedures.

Furthermore, the protocol for the experimental procedure has been already stablished (included in X-X appendix). This includes the main objectives and steps to be followed for the performance of the experiments. All information regarding the impact device, parameters, biomarkers, type of experiments and elements for the database creation are specified. As well, requirements for biological measurements are determined for the procedure.

A second objective has been to write the scientific article about the development of the impact device. It has to be said that the article has been finished but it is in the procedure to be published. As well, it is expected to write a second article denoting all the performances of the impact experiments with neural cells to show obtained results between impact properties and biological effects.

With the aim to widening studies in TBI, it has been considered to develop the same impact device but in a higher scale. Two meters high device will be developed to perform experiments with larger impact velocities. This way, it will be possible to translate the experimental scale to analyse impact effects with higher energy transfer methods.

In addition, the project development is focused to be open for new researchers. With that aim, all information, procedures and developed tasks (CAD files, computed codes, FEM, etc.) will be included in a GitHub platform. This way, the project would be accessible for sharing, easing future studies in this field.

7. References

[1] D. F. Meaney, B. Morrison, et C. Dale Bass, « The Mechanics of Traumatic Brain Injury: A Review of What We Know and What We Need to Know for Reducing Its Societal Burden », *J. Biomech. Eng.*, vol. 136, n° 2, p. 021008, févr. 2014, doi: 10.1115/1.4026364.

[2] F. E. Lecky *et al.*, « The burden of traumatic brain injury from low-energy falls among patients from 18 countries in the CENTER-TBI Registry: A comparative cohort study », *PLOS Med.*, vol. 18, n° 9, p. e1003761, sept. 2021, doi: 10.1371/journal.pmed.1003761.

[3] M. P. Alexander, « Mild traumatic brain injury: Pathophysiology, natural history, and clinical management », *Neurology*, vol. 45, n° 7, p. 1253-1260, juill. 1995, doi: 10.1212/WNL.45.7.1253.

[4] M. Sherer et A. M. Sander, Éd., *Handbook on the Neuropsychology of Traumatic Brain Injury*. New York, NY: Springer New York, 2014. doi: 10.1007/978-1-4939-0784-7.

[5] K. Blennow, J. Hardy, et H. Zetterberg, « The Neuropathology and Neurobiology of Traumatic Brain Injury », *Neuron*, vol. 76, n° 5, p. 886-899, déc. 2012, doi: 10.1016/j.neuron.2012.11.021.

[6] T. Garland, « The relation between maximal running speed and body mass in terrestrial mammals », *J. Zool.*, vol. 199, n° 2, p. 157-170, févr. 1983, doi: 10.1111/j.1469-7998.1983.tb02087.x.

[7] K. Harada, T. Kamiya, et T. Tsuboi, « Gliotransmitter Release from Astrocytes: Functional, Developmental, and Pathological Implications in the Brain », *Front. Neurosci.*, vol. 9, janv. 2016, doi: 10.3389/fnins.2015.00499.

[8] M. V. Sofroniew et H. V. Vinters, « Astrocytes: biology and pathology », *Acta Neuropathol. (Berl.)*, vol. 119, n° 1, p. 7-35, janv. 2010, doi: 10.1007/s00401-009-0619-8.

[9] E. D. Bigler, « Systems Biology, Neuroimaging, Neuropsychology, Neuroconnectivity and Traumatic Brain Injury », *Front. Syst. Neurosci.*, vol. 10, août 2016, doi: 10.3389/fnsys.2016.00055.

[10] K. Baranger *et al.*, « MT5-MMP is a new pro-amyloidogenic proteinase that promotes amyloid pathology and cognitive decline in a transgenic mouse model of Alzheimer's disease », *Cell. Mol. Life Sci.*, vol. 73, n° 1, p. 217-236, janv. 2016, doi: 10.1007/s00018-015-1992-1.

[11] D. O. Okonkwo *et al.*, « GFAP-BDP as an Acute Diagnostic Marker in Traumatic Brain Injury: Results from the Prospective Transforming Research and Clinical Knowledge in Traumatic Brain Injury Study », *J. Neurotrauma*, vol. 30, n° 17, p. 1490-1497, sept. 2013, doi: 10.1089/neu.2013.2883.

[12] R. P. Berger, « The Use of Serum Biomarkers to Predict Outcome After Traumatic Brain Injury in Adults and Children »:, *J. Head Trauma Rehabil.*, vol. 21, n° 4, p. 315-333, juill. 2006, doi: 10.1097/00001199-200607000-00004.

[13] P. M. Kochanek, R. P. Berger, H. Bayr, A. K. Wagner, L. W. Jenkins, et R. S. Clark, « Biomarkers of primary and evolving damage in traumatic and ischemic brain injury: diagnosis, prognosis, probing mechanisms, and therapeutic decision making »:, *Curr. Opin. Crit. Care*, vol. 14, n° 2, p. 135-141, avr. 2008, doi: 10.1097/MCC.0b013e3282f57564.

[14] D. P. Q. Clark *et al.*, « Inflammation in Traumatic Brain Injury: Roles for Toxic A1 Astrocytes and Microglial–Astrocytic Crosstalk », *Neurochem. Res.*, vol. 44, n° 6, p. 1410-1424, juin 2019, doi: 10.1007/s11064-019-02721-8.

[15] F. Murillo-Cabezas *et al.*, « The prognostic value of the temporal course of S100 β protein in post-acute severe brain injury: A prospective and observational study », *Brain Inj.*, vol. 24, nº 4, p. 609-619, avr. 2010, doi: 10.3109/02699051003652823.
[16] T. Rainey, M. Lesko, R. Sacho, F. Lecky, et C. Childs, « Predicting outcome after severe traumatic brain injury using the serum S100B biomarker: Results using a single (24h) time-point », *Resuscitation*, vol. 80, nº 3, p. 341-345, mars 2009, doi: 10.1016/j.resuscitation.2008.11.021.
[17] C. A. Pfortmueller *et al.*, « S-100 B Concentrations Are a Predictor of Decreased Survival in Patients with Major Trauma, Independently of Head Injury », *PLOS ONE*, vol. 11, nº 3, p. e0152822, mars 2016, doi: 10.1371/journal.pone.0152822.
[18] D. F. Meaney *et al.*, « Modification of the Cortical Impact Model To Produce Axonal Injury in the Rat Cerebral Cortex », *J. Neurotrauma*, vol. 11, nº 5, p. 599-612, oct. 1994, doi: 10.1089/neu.1994.11.599.
[19] E. Gutierrez *et al.*, « A New Model for Diffuse Brain Injury by Rotational Acceleration: I. Model, Gross Appearance, and Astrocytosis », *J. Neurotrauma*, vol. 18, nº 3, p. 247-257, mars 2001, doi: 10.1089/08977150151070874.
[20] E. F. Ellis, J. S. Mckinney, K. A. Willoughby, S. Liang, et J. T. Povlishock, « A New Model for Rapid Stretch-Induced Injury of Cells in Culture: Characterization of the Model Using Astrocytes », *J. Neurotrauma*, vol. 12, nº 3, p. 325-339, juin 1995, doi: 10.1089/neu.1995.12.325.
[21] D. M. Geddes et R. S. Cargill, « An in Vitro Model of Neural Trauma: Device Characterization and Calcium Response to Mechanical Stretch », *J. Biomech. Eng.*, vol. 123, nº 3, p. 247-255, juin 2001, doi: 10.1115/1.1374201.
[22] B. Morrison, J. H. Eberwine, D. F. Meaney, et T. K. McIntosh, « Traumatic injury induces differential expression of cell death genes in organotypic brain slice cultures determined by complementary DNA array hybridization », *Neuroscience*, vol. 96, nº 1, p. 131-139, janv. 2000, doi: 10.1016/S0306-4522(99)00537-0.
[23] J. A. Chuckowree et J. C. Vickers, « Cytoskeletal and Morphological Alterations Underlying Axonal Sprouting after Localized Transection of Cortical Neuron Axons *In Vitro* », *J. Neurosci.*, vol. 23, nº 9, p. 3715-3725, mai 2003, doi: 10.1523/JNEUROSCI.23-09-03715.2003.
[24] E. S. Tecoma, H. Monyer, M. P. Goldberg, et D. W. Choi, « Traumatic neuronal injury in vitro is attenuated by NMDA antagonists », *Neuron*, vol. 2, nº 6, p. 1541-1545, juin 1989, doi: 10.1016/0896-6273(89)90042-1.
[25] A. G. Mukhin, S. A. Ivanova, S. M. Knoblach, et A. I. Faden, « New *In Vitro* Model of Traumatic Neuronal Injury: Evaluation of Secondary Injury and Glutamate Receptor-Mediated Neurotoxicity », *J. Neurotrauma*, vol. 14, nº 9, p. 651-663, sept. 1997, doi: 10.1089/neu.1997.14.651.
[26] A. G. Mukhin, S. A. Ivanova, J. W. Allen, et A. I. Faden, « Mechanical injury to neuronal/glial cultures in microplates: Role of NMDA receptors and pH in secondary neuronal cell death », *J. Neurosci. Res.*, vol. 51, nº 6, p. 748-758, mars 1998, doi: 10.1002/(SICI)1097-4547(19980315)51:6<748::AID-JNR8>3.0.CO;2-B.
[27] A. Laskowski, W. Schmidt, K. Dinkel, M. Martínez-Sánchez, et K. G. Reymann, « bFGF and EGF modulate trauma-induced proliferation and neurogenesis in juvenile organotypic hippocampal slice cultures », *Brain Res.*, vol. 1037, nº 1-2, p. 78-89, mars 2005, doi: 10.1016/j.brainres.2004.12.035.
[28] J. W. Allen, S. M. Knoblach, et A. I. Faden, « Combined mechanical trauma and metabolic impairment *in vitro* induces NMDA receptor-dependent neuronal cell death and caspase-3-dependent apoptosis », *FASEB J.*, vol. 13, nº 13, p. 1875-1882, oct. 1999, doi: 10.1096/fasebj.13.13.1875.

[29] A. Faden, V. Movsesyan, S. Knoblach, F. Ahmed, et I. Cernak, « Neuroprotective effects of novel small peptides in vitro and after brain injury », *Neuropharmacology*, vol. 49, n° 3, p. 410-424, sept. 2005, doi: 10.1016/j.neuropharm.2005.04.001.
[30] F. Sieg, P. Wahle, et H.-C. Pape, « Cellular Reactivity to Mechanical Axonal Injury in an Organotypic *in Vitro* Model of Neurotrauma », *J. Neurotrauma*, vol. 16, n° 12, p. 1197-1213, déc. 1999, doi: 10.1089/neu.1999.16.1197.
[31] A. J. Church et R. D. Andrew, « Spreading Depression Expands Traumatic Injury in Neocortical Brain Slices », *J. Neurotrauma*, vol. 22, n° 2, p. 277-290, févr. 2005, doi: 10.1089/neu.2005.22.277.
[32] T. A. Gennarelli, L. E. Thibault, J. H. Adams, D. I. Graham, C. J. Thompson, et R. P. Marcincin, « Diffuse axonal injury and traumatic coma in the primate », *Ann. Neurol.*, vol. 12, n° 6, p. 564-574, déc. 1982, doi: 10.1002/ana.410120611.
[33] A. I. King, J. S. Ruan, C. Zhou, W. N. Hardy, et T. B. Khalil, « Recent Advances in Biomechanics of Brain Injury Research: A Review », *J. Neurotrauma*, vol. 12, n° 4, p. 651-658, août 1995, doi: 10.1089/neu.1995.12.651.
[34] M. Bottlang, M. B. Sommers, T. A. Lusardi, J. J. Miesch, R. P. Simon, et Z.-G. Xiong, « Modeling Neural Injury in Organotypic Cultures by Application of Inertia-Driven Shear Strain », *J. Neurotrauma*, vol. 24, n° 6, p. 1068-1077, juin 2007, doi: 10.1089/neu.2006.3772.
[35] M. C. LaPlaca, D. K. Cullen, J. J. McLoughlin, et R. S. Cargill, « High rate shear strain of three-dimensional neural cell cultures: a new in vitro traumatic brain injury model », *J. Biomech.*, vol. 38, n° 5, p. 1093-1105, mai 2005, doi: 10.1016/j.jbiomech.2004.05.032.
[36] B. Morrison, B. S. Elkin, J.-P. Dollé, et M. L. Yarmush, « In Vitro Models of Traumatic Brain Injury », *Annu. Rev. Biomed. Eng.*, vol. 13, n° 1, p. 91-126, août 2011, doi: 10.1146/annurev-bioeng-071910-124706.
[37] K. L. Panizzon, D. Shin, S. Frautschy, et R. A. Wallis, « Neuroprotection with Bcl-220–34 peptide against trauma »:, *NeuroReport*, vol. 9, n° 18, p. 4131-4136, déc. 1998, doi: 10.1097/00001756-199812210-00024.
[38] M. Koshinaga, Y. Katayama, M. Fukushima, H. Oshima, T. Suma, et T. Takahata, « Rapid and Widespread Microglial Activation Induced by Traumatic Brain Injury in Rat Brain Slices », *J. Neurotrauma*, vol. 17, n° 3, p. 185-192, mars 2000, doi: 10.1089/neu.2000.17.185.
[39] Y. Etzion et Y. Grossman, « Pressure-induced depression of synaptic transmission in the cerebellar parallel fibre synapse involves suppression of presynaptic N-type Ca $^{2+}$ channels: Parallel fibre synapse at pressure », *Eur. J. Neurosci.*, vol. 12, n° 11, p. 4007-4016, nov. 2000, doi: 10.1046/j.1460-9568.2000.00303.x.
[40] H. L. Cater, L. E. Sundstrom, et B. Morrison, « Temporal development of hippocampal cell death is dependent on tissue strain but not strain rate », *J. Biomech.*, vol. 39, n° 15, p. 2810-2818, janv. 2006, doi: 10.1016/j.jbiomech.2005.09.023.
[41] H. L. Cater, D. Gitterman, S. M. Davis, C. D. Benham, B. Morrison, et L. E. Sundstrom, « Stretch-induced injury in organotypic hippocampal slice cultures reproduces in vivo post-traumatic neurodegeneration: role of glutamate receptors and voltage-dependent calcium channels », *J. Neurochem.*, vol. 101, n° 2, p. 434-447, avr. 2007, doi: 10.1111/j.1471-4159.2006.04379.x.
[42] Z. Yu et B. Morrison, « Experimental Mild Traumatic Brain Injury Induces Functional Alteration of the Developing Hippocampus », *J. Neurophysiol.*, vol. 103, n° 1, p. 499-510, janv. 2010, doi: 10.1152/jn.00775.2009.

[43] P.-A. Buchs, L. Stoppini, et D. Muller, « Structural modifications associated with synaptic development in area CA1 of rat hippocampal organotypic cultures », *Dev. Brain Res.*, vol. 71, nº 1, p. 81-91, janv. 1993, doi: 10.1016/0165-3806(93)90108-M.
[44] O. Robain, G. Barbin, Th. Billette de Villemeur, L. Jardin, Th. Jahchan, et Y. Ben-Ari, « Development of mossy fiber synapses in hippocampal slice culture », *Dev. Brain Res.*, vol. 80, nº 1-2, p. 244-250, juill. 1994, doi: 10.1016/0165-3806(94)90109-0.
[45] C. Collin, K. Miyaguchi, et M. Segal, « Dendritic Spine Density and LTP Induction in Cultured Hippocampal Slices », *J. Neurophysiol.*, vol. 77, nº 3, p. 1614-1623, mars 1997, doi: 10.1152/jn.1997.77.3.1614.
[46] D. K. Cullen, C. M. Simon, et M. C. LaPlaca, « Strain rate-dependent induction of reactive astrogliosis and cell death in three-dimensional neuronal–astrocytic co-cultures », *Brain Res.*, vol. 1158, p. 103-115, juill. 2007, doi: 10.1016/j.brainres.2007.04.070.
[47] Y. Nakayama, Y. Aoki, et H. Niitsu, « Studies on the Mechanisms Responsible for the Formation of Focal Swellings on Neuronal Processes Using a Novel *In Vitro* Model of Axonal Injury », *J. Neurotrauma*, vol. 18, nº 5, p. 545-554, mai 2001, doi: 10.1089/089771501300227341.
[48] G. Serbest, J. Horwitz, et K. Barbee, « The Effect of Poloxamer-188 on Neuronal Cell Recovery from Mechanical Injury », *J. Neurotrauma*, vol. 22, nº 1, p. 119-132, janv. 2005, doi: 10.1089/neu.2005.22.119.
[49] B. J. Pfister, T. P. Weihs, M. Betenbaugh, et G. Bao, « An In Vitro Uniaxial Stretch Model for Axonal Injury », *Ann. Biomed. Eng.*, vol. 31, nº 5, p. 589-598, mai 2003, doi: 10.1114/1.1566445.
[50] E. Bar-Kochba, M. T. Scimone, J. B. Estrada, et C. Franck, « Strain and rate-dependent neuronal injury in a 3D in vitro compression model of traumatic brain injury », *Sci. Rep.*, vol. 6, nº 1, p. 30550, août 2016, doi: 10.1038/srep30550.
[51] S. Koumlis, H. Cheng, T. E. Morgan, C. E. Finch, et V. Eliasson, « Glial Model for Traumatic Brain Injury: Network Strain Field and Inflammation Induced by Repeated Mechanical Impacts In Vitro », *Exp. Mech.*, vol. 58, nº 1, p. 125-135, janv. 2018, doi: 10.1007/s11340-017-0338-3.
[52] W. S. Hoogenboom *et al.*, « Diffusion Tensor Imaging of the Evolving Response to Mild Traumatic Brain Injury in Rats », *J. Exp. Neurosci.*, vol. 13, p. 117906951985862, janv. 2019, doi: 10.1177/1179069519858627.
[53] « Norme Casque Vélo.pdf ».

Appendix

A -1 Specifications

The aim of specifications is to gather all the information and requirements to complete the objectives of the project. For that, general working conditions and resources are described in this annexe. In this project to complete the master thesis a shock cell device has been developed and manufactured in order to analyse impact effects on neural cells and genetically modified Alzheimer's disease neural cells. Agreed deadline has been determined for six months, starting in October of 2021 and finishing in March of 2022. The development of this project will help to overcome the actual frontiers in brain impact science and contribute to further studies of impacts on large heads in an original manner.

Resources

Several resources and materials have been necessary for the development of the project including:

- Raw material for cell shock prototype manufacturing
  - Steel
  - Rubber
- Cells
  - Neural cells (generated from embryonic E16 C57BL/6 mice)
  - Genetically modified AD cells ()
- Petry dishes (24 wells)
- IEPE Accelerometers
- DAQ (Labjack)
- Raspberry Pi 4

Equipment used is the next:

- 3D printer for mouldings of the bumper
- Workshop → CNC machine, lathe
- Sterile chamber (Sterile Laminar flow hood)
- HCS microscopy
- Elisa testing

Software:

- Mathematical software MATLAB for calculus of maximum acceleration and contact times.
- 3D Experience software for design of the cell shock device and following FEM analysis.
- Phyton software for characterisation of acquired data from accelerometers.
- Nodered for experiment automation
- Latex for scientific paper writing

Security

Not relevant

Waste management

Not relevant

A-2 Timone hospital experiments protocol

This document has been written for the CASSIS project of a new embedded system for head-impact injury prediction during the phase of experimentation. The new manufactured shock-cell impactor developed by P1, and biological elements (mixed neural/glial cells) obtained from P2 will be combined to implement a standardized controlled impact tests on a neural cell model.

The following protocol details all the specifications and requirements regarding proposed objectives. Specific tasks and steps must be followed when manipulating laboratory goods (fluids, cells, antigens, etc.) and experiments will be performed in extremely precision and precaution.

The characteristics of the device have been included in order to ensure good manipulation of the same.

1. Where / when

The experiments will start on April in the Universitary Hospital of Timone in Marseille. The experiments will be performed in the laboratories of the Institute of NeuroPathophysiology (INP-CNRS/AMU).

The manufactured device will be moved on to the TIMONE's laboratories at the beginning of the experimental phase and will be preserved in a specific space for proper working environment. All the elements for device disposition and set up will be

provided by P1, this includes all the mounting elements, tools, replacement parts, electronic devices, etc.

The device must be placed in a rigid stable platform in order to avoid non desired vibrations. Otherwise, it requires enough space to place all the electronic devices for data acquisition during the experimental process. A drawer was discussed as a platform.

If working space must be changed, the compact design of the device enables an easy transport of the same without any inconveniences.

2. Objectives

The main objective is to implement a standardized controlled impact tests on a neural cell model. Quantitative and qualitative measurement will be carried out:

- Biochemical measures
- Immunocytochemical and morphological assessment
- Determined biomarker and impact parameters will be represented graphically
- Creation of database to record analysed biomarkers and impact parameters data

Previously, the functionality of the device will be validated for work with cell cultures.

3. Specifications

3.1. Device

The compact design of the impactor has been developed to be easy to manipulate (transport, loading, height position selection, etc.) and enables to reproduce the experiments as many times as required. The device will be placed at selected space and will be possible to be used for any worker involved in the experiments as it does require little training knowledge for its manipulation.

3.2. Parameters

The combination of selected bumper and height position will result in different maximum acceleration and contact time of the impact. The proposed experiments will be performed by following parameters:

a.) Bumpers (6 in total)

- Young's modulus of 10 MPa
    - R = 50 mm, 300 mm, and 1000 mm.

- Young's modulus of 100 MPa
    - R = 50 mm, 300 mm, and 1000 mm.

b.) <u>Height position</u> (related to impact velocities)

- 30 cm → 2.4 m/s
- 25 cm → 2.2 m/s
- 20 cm → 2 m/s
- 15 cm → 1.7 m/s
- 10 cm → 1.4 m/s

c.) <u>Maximum acceleration and contact time</u>

Regarding previous testing experiments, obtained maximum acceleration values are given in a range between 0 and 1600 m/s² and contact time (impact duration) between 0 and 10 ms.

3.3. Biomarkers

For this study, four different biomarkers will be analysed: **(discuss with Santiago)**

- βIII-tubulin → neural viability related
- GFAP → glial inflammatory response
- S-100β → glial inflammatory response

3.4. Experiments performance

The proposed experiments include following ones:

- Same culture in different bumpers and same height – ONE IMPACT
- Same culture in different bumpers and same height – SEVERAL IMPACTS
- Same culture in different bumpers and different height – ONE IMPACT
- Same culture in different bumpers and different height – SEVERAL IMPACTS
- Different cultures (cell density, antigens, etc.) and same procedures above.

Considering previously mentioned elements, it has been decided to perform two kind of experiments (one impact and several impacts) involving four biomarkers, with six different bumpers and in all five heights. In addition, for biological assessment, it has been decided to reproduce each cycle of performances three times.

Therefore, in total we estimate to perform **360** experiments (**6 bumpers x 5 height x 4 biomarkers x 3 reproductions**) for those involving one impacts.

For experiments involving several impacts, the number of experiments will be **multiplied in function** of decided number of impacts. A waiting period of **2h** is placed between impacts.

Before performing the real experiments, some verification tries will be performed to determine if the cell cultures remain in good state in each situation. We will confirm that every height (impact velocities) and corresponding acceleration effects are available for the experiments and do not destroy cell cultures and used materials. Also, every bumper will be testes to verify the workability of the same.

3.5. Database

To organize the database creation, varied parameters will be recorded:

- Maximum acceleration
- Contact time
- Height
- Impact velocity
- Young's modulus of the bumper (specific for each one)
- Radius of curvature of the bumper (specific for each one)
- Biomarkers
- Type and number of cell culture
- Type of experiment
- Number of the experiment
- Cycle of testing (experiments are reproduced 3 times)
- Date / time

All information will be placed in the same document to ease data extraction, treatment, and future processing. The goal is to perform statistical analysis of the results obtained from the experiments and enhance most valuable conclusions.

4. Requirements

4.1. Measurements

a. HCS
   i. βIII-tubulin, MAP-2, caspase 3, MTT test
   ii. PSD95, Synaptophysin
   iii. GFAP, S-100β, Iba1
b. ELISA
   i. Pro-inflammatory cytokines
   ii. AD-linked β amyloid peptide (Aβ40 an Aβ42)

Based on literature, to investigate the inflammatory response biomarkers are going to be measure **4h** after the impacts[1]. Otherwise, it has been shown that due to compressive strains, some morphological effects such as blebs can appear. Regarding Bar-Kochba et al. [2], **6h** after impacts blebs starts and from **7h to 12h** cell death can occur. It is interesting to make a following every two hours to study every change in the cultures.

Cultures exposed to several impacts will be measured **4h after last impact**.

4.2. Cell cultures

All cell cultures must be preserved in a sterile environment. For that, prepared cultures will be moved from sterile laboratory to the device just in cases where experiments will be carried out. At the same time, cell cultures must be return to sterile environment as soon as possible to preserve its nature. Cell culture manipulation and displacement will be performed in function of requirements stablished for experiment specifications (measure times, culture maturation, etc.).

4.3. Materials

c. Laboratory materials
    i. Ø40 mm Millicell petri-dish.
    ii. Etc.
d. Liquids / fluids
    i. Fluids for cell/glial conservation
    ii. Etc.

4.4. Biologic elements

- Mixed neural/glial cells from embryonic E16C57BL/6 mice
- Astrocytes
- Antigens??

5. Staining

(TO BE CONTRASTED WITH TIMONE HOSPITAL TEAM)

6. Culture preparation

(TO BE CONTRASTED WITH TIMONE HOSPITAL TEAM)

7. References

[1] S. Koumlis, H. Cheng, T. E. Morgan, C. E. Finch, y V. Eliasson, «Glial Model for Traumatic Brain Injury: Network Strain Field and Inflammation Induced by Repeated Mechanical Impacts In Vitro», *Exp. Mech.*, vol. 58, n.º 1, pp. 125-135, ene. 2018, doi: 10.1007/s11340-017-0338-3.

[2] E. Bar-Kochba, M. T. Scimone, J. B. Estrada, y C. Franck, «Strain and rate-dependent neuronal injury in a 3D in vitro compression model of traumatic brain injury», *Sci. Rep.*, vol. 6, n.º 1, p. 30550, ago. 2016, doi: 10.1038/srep30550.

A-3 CAD files

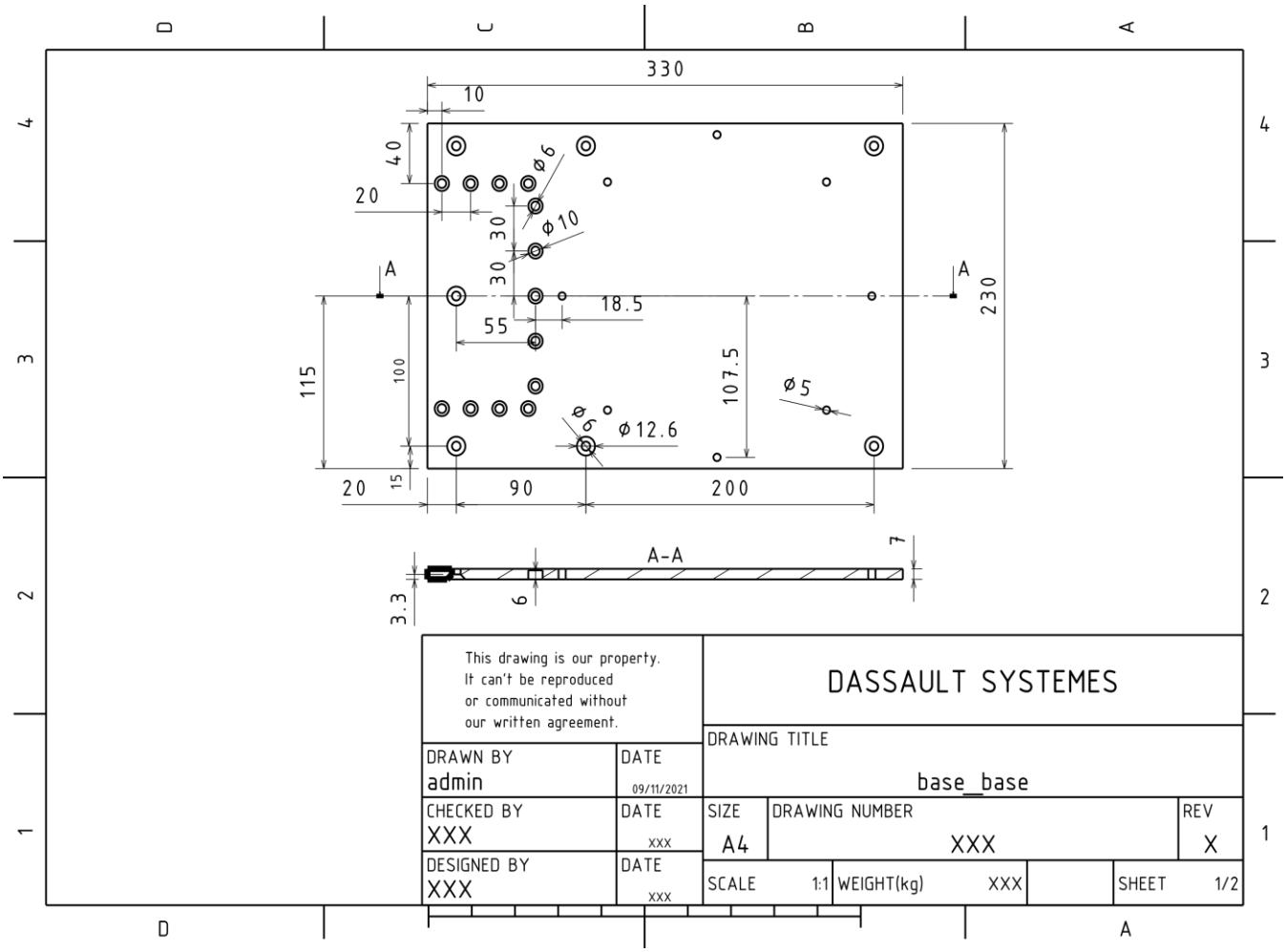
330
10
40
20
30
30
ø6
ø10
A
A
18.5
55
230
115
100
107.5
ø5
ø6
ø12.6
20
15
90
200
A-A
7
3.3
6
This drawing is our property.
It can't be reproduced
or communicated without
our written agreement.
DASSAULT SYSTEMES
DRAWN BY
admin
DATE
09/11/2021
DRAWING TITLE
base_base
CHECKED BY
XXX
DATE
XXX
SIZE
A4
DRAWING NUMBER
XXX
REV
X
DESIGNED BY
XXX
DATE
XXX
SCALE
1:1
WEIGHT(kg)
XXX
SHEET
1/2

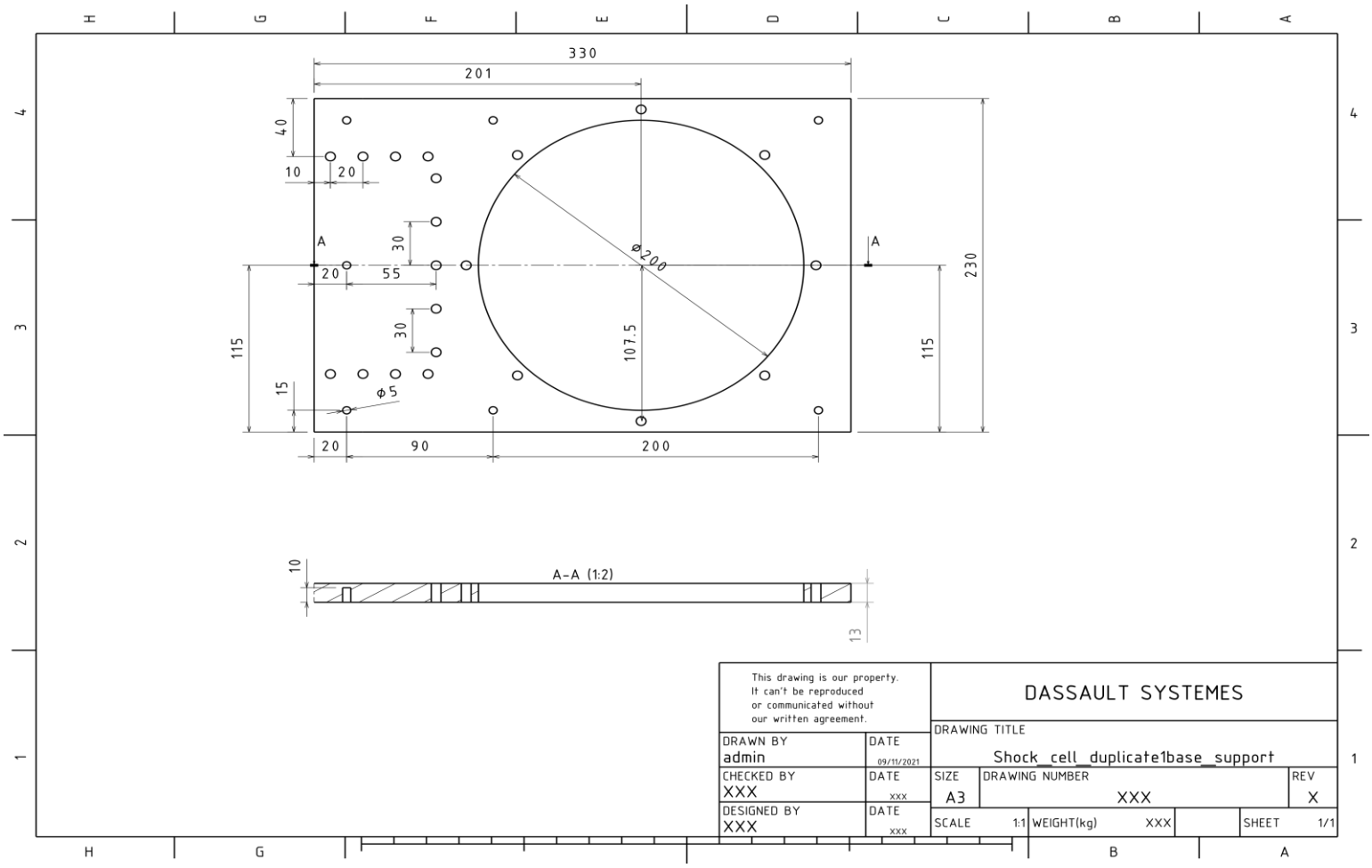
330
201
40
10
20
A
30
20
55
ø200
A
230
115
30
107.5
115
15
ø5
20
90
200
A-A (1:2)
10
13
This drawing is our property.
It can't be reproduced
or communicated without
our written agreement.
DASSAULT SYSTEMES
DRAWN BY
admin
DATE
09/11/2021
DRAWING TITLE
Shock_cell_duplicate1base_support
CHECKED BY
XXX
DATE
XXX
SIZE
A3
DRAWING NUMBER
XXX
REV
X
DESIGNED BY
XXX
DATE
XXX
SCALE
1:1
WEIGHT(kg)
XXX
SHEET
1/1

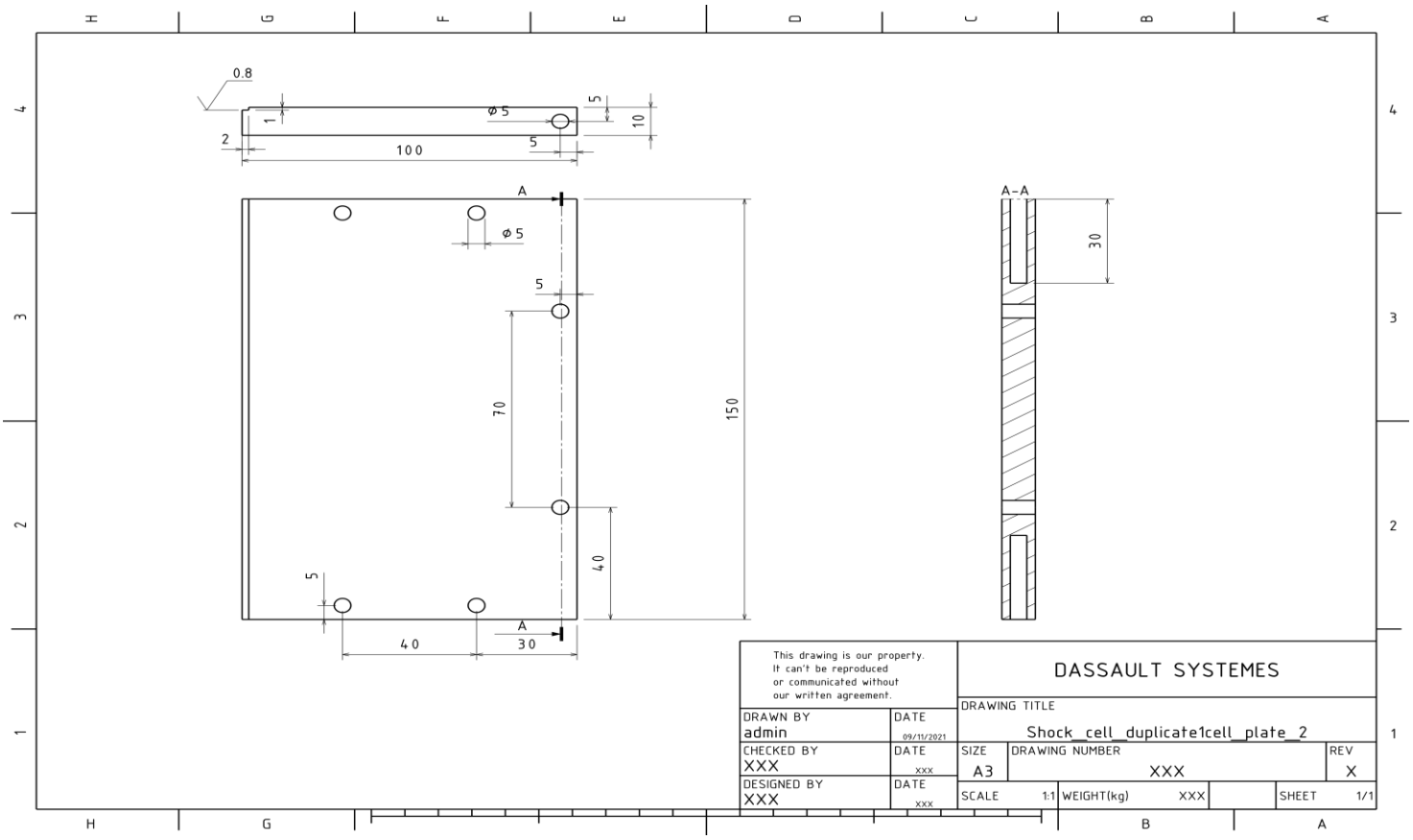
0.8
1
2
100
5
10
5
ø5
A
ø5
5
70
150
40
5
40
30
A
A-A
30
This drawing is our property.
It can't be reproduced
or communicated without
our written agreement.
DASSAULT SYSTEMES
DRAWN BY
admin
DATE
09/11/2021
DRAWING TITLE
Shock_cell_duplicate1cell_plate_2
CHECKED BY
XXX
DATE
XXX
SIZE
A3
DRAWING NUMBER
XXX
REV
X
DESIGNED BY
XXX
DATE
XXX
SCALE
1:1
WEIGHT(kg)
XXX
SHEET
1/1

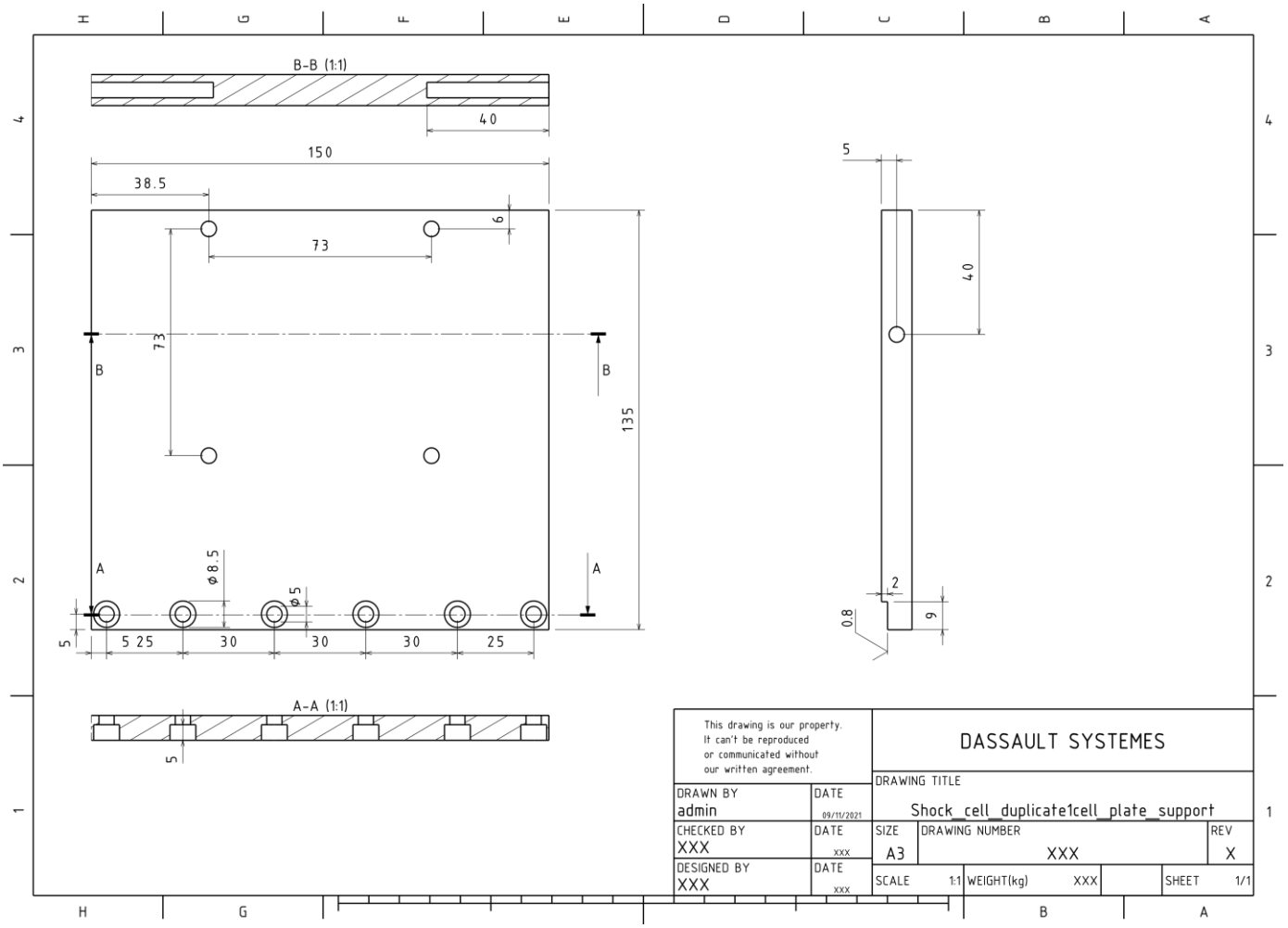
B-B (1:1)
40
150
38.5
73
6
73
135
B
B
A
A
ϕ8.5
ϕ5
5
5 25
30
30
30
25
A-A (1:1)
5
5
40
2
9
0.8
This drawing is our property.
It can't be reproduced
or communicated without
our written agreement.
DASSAULT SYSTEMES
DRAWING TITLE
Shock_cell_duplicate1cell_plate_support
DRAWN BY
admin
DATE
09/11/2021
CHECKED BY
XXX
DATE
XXX
DESIGNED BY
XXX
DATE
XXX
SIZE
A3
DRAWING NUMBER
XXX
REV
X
SCALE
1:1
WEIGHT(kg)
XXX
SHEET
1/1

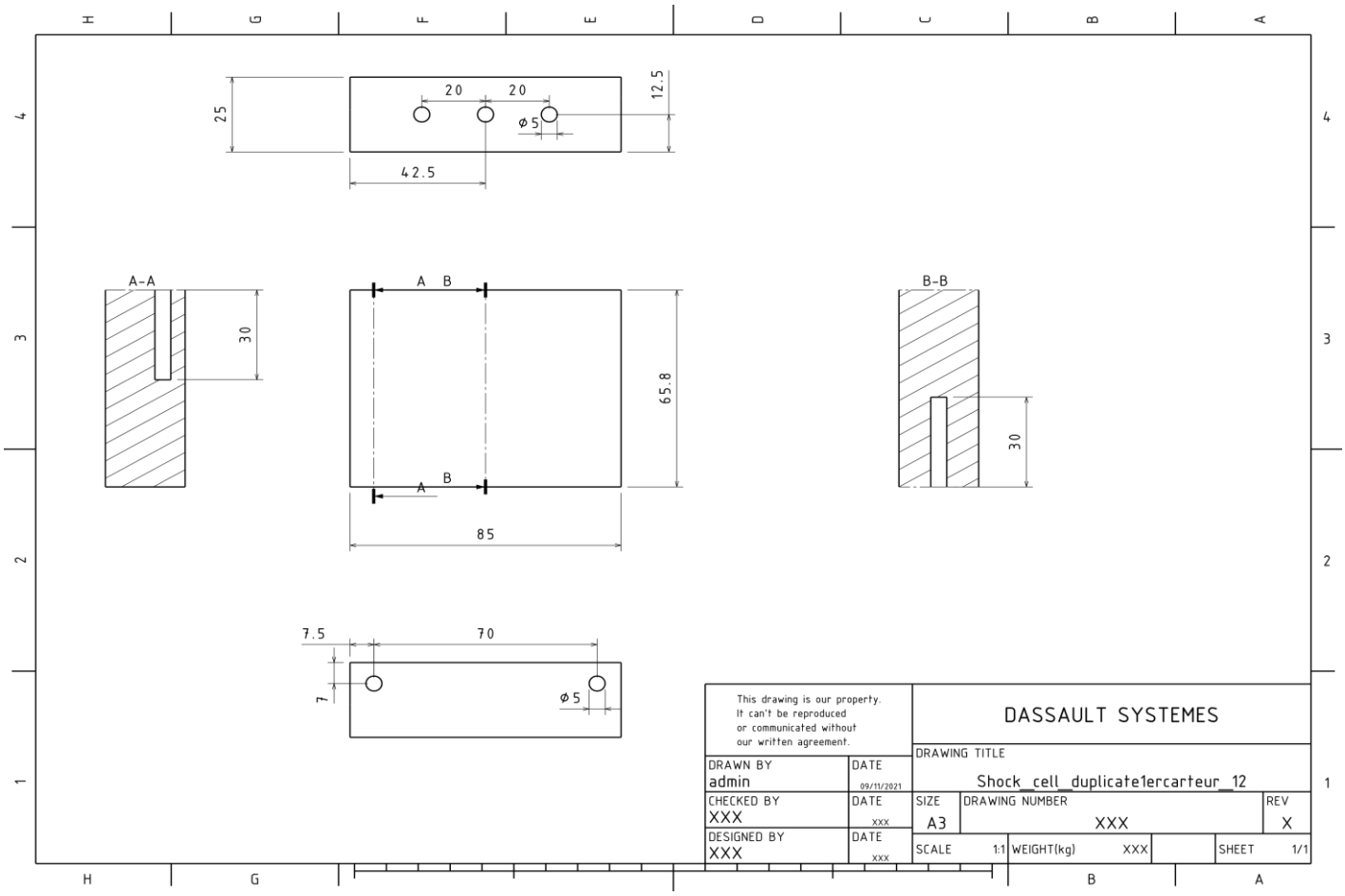
20
20
12.5
25
ø5
42.5
A-A
30
A B
65.8
B
A
85
B-B
30
7.5
70
7
ø5
This drawing is our property.
It can't be reproduced
or communicated without
our written agreement.
DASSAULT SYSTEMES
DRAWN BY
admin
DATE
09/11/2021
DRAWING TITLE
Shock_cell_duplicate1ercarteur_12
CHECKED BY
XXX
DATE
XXX
SIZE
A3
DRAWING NUMBER
XXX
REV
X
DESIGNED BY
XXX
DATE
XXX
SCALE
1:1
WEIGHT(kg)
XXX
SHEET
1/1

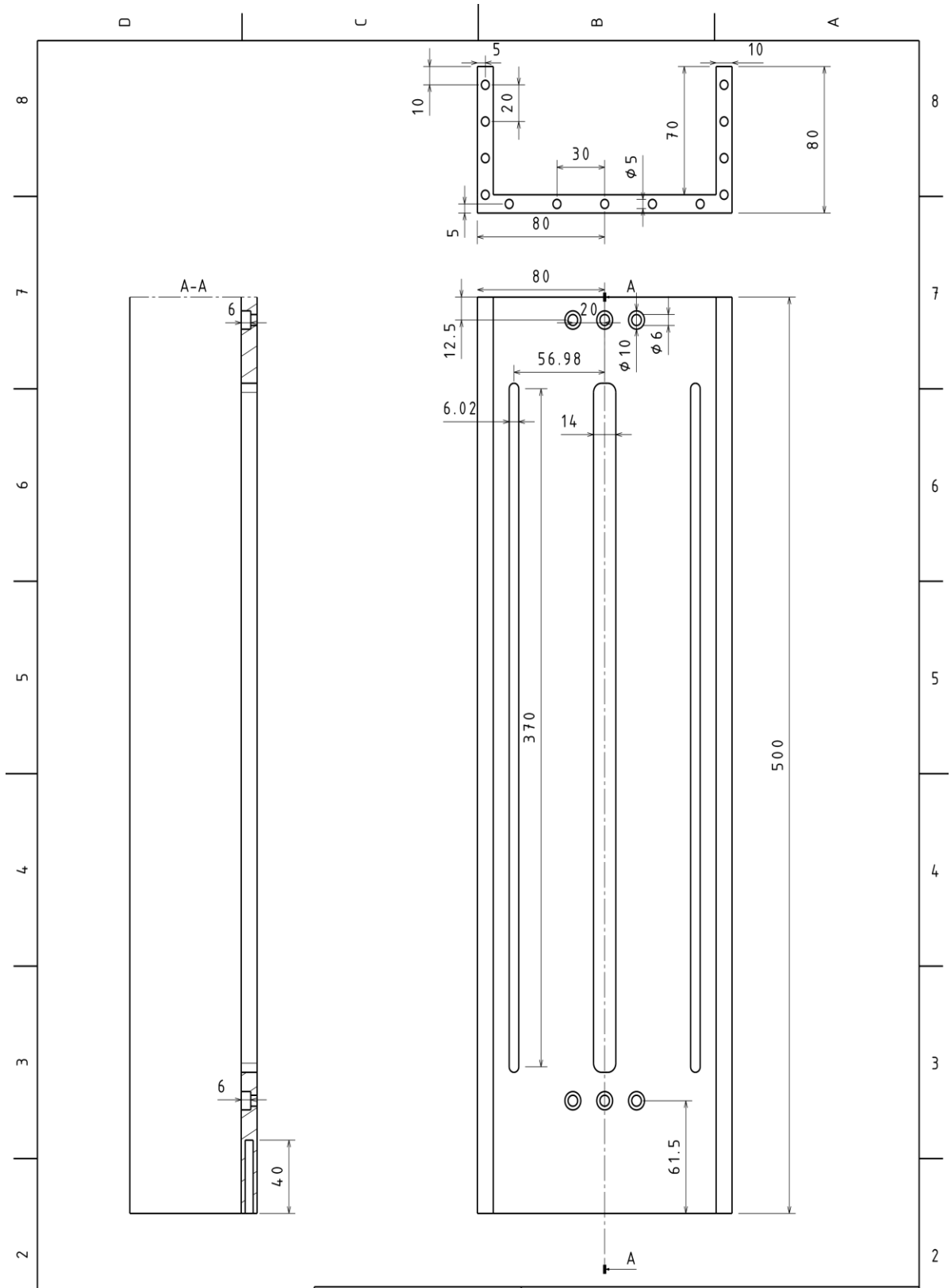

This drawing is our property. It can't be reproduced or communicated without our written agreement.		DASSAULT SYSTEMES			
DRAWN BY admin	DATE 09/11/2021	DRAWING TITLE Shock_cell_duplicate1Beam_support			
CHECKED BY XXX	DATE XXX	SIZE A3	DRAWING NUMBER XXX		REV X
DESIGNED BY XXX	DATE XXX	SCALE 1:1	WEIGHT(kg) XXX		SHEET 1/1

A-4 Article for publication

The article is finished in process of correction. It is expected to be finished in the next few weeks to start the arrangement for publishing.

Biomedical_Engineering_2022_03_30.pdf